POLITECNICO DI TORINO

I Facoltà di Ingegneria

Corso di Laurea in Ingegneria Energetica e Nucleare

Master of Science Thesis

Making synthetic fuels for the industrial sector via solid oxide electrolysis and catalytic upgrade using recovered carbon dioxide and residual biomass

Advisor:

Prof. Ing. Massimo Santarelli

Candidate:

Mattia PALUMBO

Academic Year 2017-2018

Index

Abstract

Nowadays the interest in the research for new fuels has become a key target in the framework of the independence from fossil fuels. In this work, a feasibility study on the substitution of natural gas in the industrial sector on a regional base with synthetic natural gas (SNG) and hydrogen has been done. Different pathways for the production of SNG have been analysed; as regards to the production of hydrogen, only one pathway has been studied. Moreover, for each pathway one or more scenarios have been investigated, and in the end a comparison of all the scenarios has been made.

In chapter 1 an introduction on the main topics treated in this work has been done, including, among others, an overview on the power-to-gas concept and the state of the art of the use of hydrogen as a fuel.

In chapter 2 a general overview on electrolysis has been done: in particular, a theoretical analysis, such as thermodynamics, and practical analysis, such as state of the art of the SOECs, have been studied.

In chapter 3 the methanation topic has been treated: aside from the thermodynamics of the process, also the description of a real methanation plant (on which the methanation modeling of this work is based) has been provided.

In chapter 4 a description of the design of the plant models developed on commercial software Aspen Plus™ has been reported.

In chapter 5 the method used for the purposes of this work has been showed, and all the data needed to develop the results have been listed.

In chapter 6 all the results of all the scenarios considered have been showed and critically commented.

1. Introduction

In the course of the most recent decades, severe economic and environmental constraints have shown up on worldwide hydrocarbon-based energy economy. So the growing energy demand and the environmental issues have led to the developing of fuels that can somehow replace the fossils ones. One promising option is hydrogen, which itself presents quite a lot of advantages.

"Low-cost hydrogen will foster a new era of energy sustainability, based on hydrogen." [1]

Its capability for transforming zero-carbon electricity sources into the supply of zero-carbon hydrogen and oxygen for heterogeneous end uses has pulled in re-established consideration during the last years, and numerous innovative development programs have been started in many nations in order to grow new incorporated advances for the management of sustainable power sources.

The other option is the production of synthetic fuels by using CO_2 either as a result of biomass gasification/biogas upgrade or from the recovering from the exhaust of fossil-fueled power plants. The last solution is good even from the perspective of a reduction of greenhouse gases (GHG) emissions.

In this context, in order to have production of synfuels in a sustainable and environmental-friendly way, electric energy produced by variable renewable sources (V-RES) appears to be a good mean to achieve the result; furthermore this type of electric energy is more difficult to dispatch compared to conventional power sources: being the option of electric energy storage a limited resource, in the last years an increased interest in alternative conversion technologies which can be sited anywhere in the world emerged.

The synfuels considered in this work have been H_2 and synthetic natural gas (SNG): the starting point of the production of both has been high-temperature solid oxide electrolytic cells (SOEC); the first one is produced through simple water electrolysis, while the second one is produced by the conversion through various steps of methanation of the syngas (H_2/CO mixture) which is a product of the co-electrolysis of H_2O and CO_2. The electricity from V-RES, in these cases, is used to drive the

electrolysis process, that represents the major expenditure in terms of energy to be provided, the auxiliary parts (compressors or pumps), and the different processes of biogas upgrading that will be subsequently mentioned.

SNG could be used in principle as easily distributed fuel for residential and industrial applications [2]. On the other hand, hydrogen in the next years could become more competitive than the natural gas of fossil origin, thank to, as said before, the electric energy from the V-RES. In fact, according to the forecasts of International Energy Agency (IEA), the price of natural gas of fossil origin will change from 0.017 €/kWh of 2020 to 0.041 €/kWh of 2040, while in the same year the cost of the hydrogen would be around 0.02÷0.03 €/kWh [3].

As said before, in this work the production of SNG through three different pathways and hydrogen through steam electrolysis has been investigated. In particular, the Italian scenario, especially the industrial sector, has been analyzed on a regional scale, considering for each region the natural gas consumption, the V-RES availability, the different resources needed and different CO_2 sources. All technologies analyzed in this work have reached at least the pre-commercial status. About hydrogen, over the past 20 years new companies have appeared on the market, and new projects have been established [4]. Gasification and methanation technologies are also fully mature [5] [6].

The aim of this work is to study the technical feasibility based on input/output energy data of a substantial introduction of synthetic gaseous fuels (SNG and H_2) in place of fossil fuel in the industrial sector of Italy on regional scale, starting from models and methods used by Monaco et al. (2018) for the transportation sector.

1.1 Overview on Power-to-Gas concept

Power-to-Gas (PTG) concept contains in it all the technologies capable of converting electrical energy to a gaseous fuel which could be hydrogen-rich gases or methane rich-gases. As can be seen in figure 1 the first step is the electrolysis process, where the electric energy necessary to drive the process can be supplied either from the V-RES or from the grid. After that the produced hydrogen can be used for different

purposes: it can be used to produce methane, or directly used in industry or mobility fields or again for heating requirements. There is the possibility to inject hydrogen directly in the gas grid, but there is a limit to this: 6% vol and the current factual fraction being around 2% vol [7].

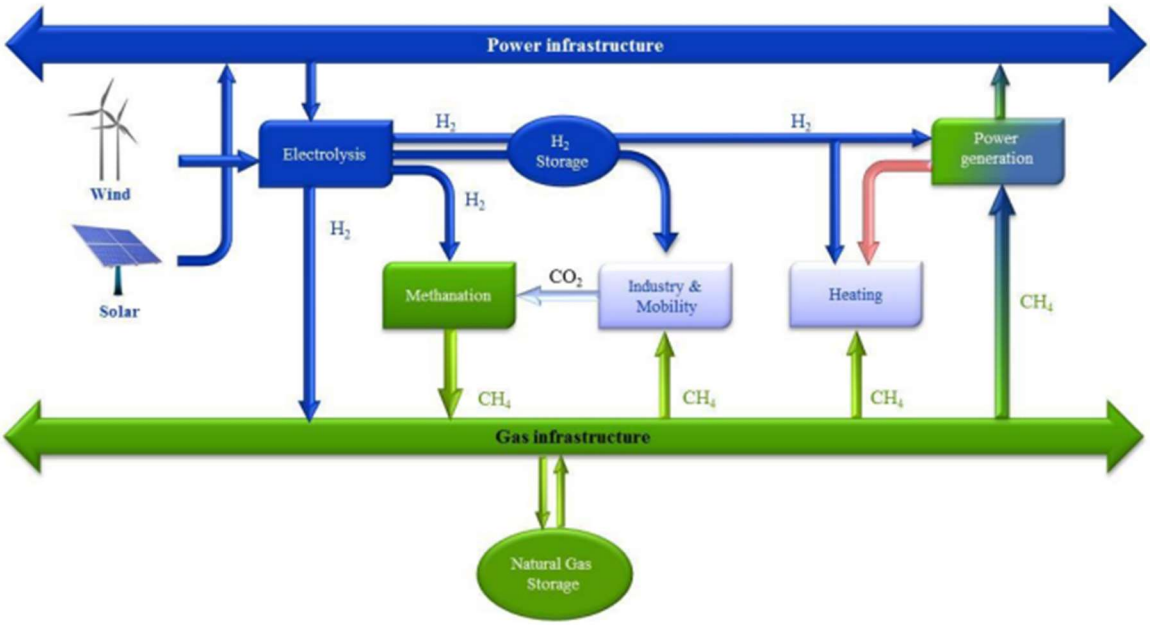

Figure 1. *Schematic description of Power-to-Gas concept* [8]

Generally, is preferable to use the produced hydrogen to produce in turn methane by methanation for many reasons:

- methane has a higher energy density with respect to hydrogen but also its flammability limits are more reduced, and it also has a higher Minimum Injection Energy (MIE) [9];
- SNG already has an existing infrastructure that covers already all Europe, while hydrogen does not have any;
- it is an almost "carbon-neutral" way to produce natural gas since the carbon dioxide used to produce syngas that afterwards will be turned into the natural gas itself is part of the carbon dioxide "sequestrated" from that emitted during of combustion of natural gas so produced.

1.2 State of the art of hydrogen as a fuel

The aim of the studies involving the use of hydrogen as a fuel has been the production of a technical solution to the problem of producing energy completely free of fossil fuels. The pros of the hydrogen as a fuel are mainly from an environmental point of view: in fact, with respect to the fossil fuels (whose combustion produces massive amounts of carbon dioxide, dangerous not only because it is a greenhouse gas, but also cause of acid rains), the hydrogen's only waste or by-product is pure water. According to the United States Department of Energy Office of Power, the most limiting problem of the use of hydrogen as a fuel is the energy that has to be provided to produce it and to overcome the energy losses in the hydrogen-to-application chain.

[…] Hydrogen requires at least twice as much energy as electricity twice the tonnage of coal, twice the number of nuclear plants, or twice the field of PV panels to perform an equivalent unit of work. Most of today's hydrogen is produced from natural gas, which is only an interim solution since it discards 30% of the energy in one valuable but depletable fuel (natural gas) to obtain 70% of another (hydrogen). The challenge is to develop more appropriate methods based on sustainable energy sources, methods that do not employ electricity as an intermediate step. […] [10]

The most cost-efficient method to produce hydrogen is steam hydrocarbon reforming, where natural gas is treated with high-temperature steam, causing a chemical breakdown of the natural gas releasing hydrogen. However, even this solution that is the best one is not nearly competitive with gasoline or natural gas.

Several alternative methods have been explored in order to lower the cost of manufacturing of the hydrogen. One promising technology is the so-called solar hydrogen: this refers to all methods of production that imply the use of the solar power to produce and collect usable hydrogen. This energy can be used in various ways to reach the final goal, such as applying the collected energy to a Stirling-cycle heat engine, which in turn drives an electricity generator to drive an electrolysis system or directly use this energy to directly "withdraw" hydrogen from hydrogen bearing sources [11].

There are also photobiological options to produce hydrogen that do not involve the use of electricity.

The use of hydrogen as a fuel and the benefits arising from this choice are analyzed in the work of Peantong et al. [12]. In this work the possibility of using a boiler that base on hydrogen as the main power is introduced. Nevertheless, there must be different requirements:

- selection of boiler with a high turndown ratio (that is the ratio between the maximum capacity to minimum capacity of the boiler);
- selection of boiler with three mode operation such as natural gas mode, H_2 mode and mixed mode;
- determination of ratio for balance hydrogen gas and natural gas in case of mixed mode.

This study shows, through experimental results, that hydrogen could be used as a substitute energy source decreasing not only the energy cost but also the level of NO_x and CO_2 release to the air.

As said before, there is not an infrastructure for the distribution of the hydrogen, even if pipelines carrying natural gas could also be able of delivering hydrogen gas, and these two gases can even be dispatched together and separated at the point of use [11]. Because of this limitation, in this work both the production and exploitation of the hydrogen as a fuel have been theoretically considered on site, i.e. a plant that has on-site both a device for the production of hydrogen (SOEC) and a boiler with the requirements listed before.

2. Fundamentals on electrolysis

The reactions of dissociation of water and carbon dioxide, as we will discuss numerically later, are not spontaneous and so it has to be provided energy to drive the reactions. The reaction can thus be driven by providing energy to the system, for instance electricity, and the device used to drive the process is called electrolyzer. An electrochemical cell basically consists of the following components:

- anode: electrode where oxidation semi-reaction take place;
- cathode: electrode where reduction semi-reaction take place;
- electrolyte: it is the medium that separates the two electrodes and allows the ionic transfer.

The electrolyte consists of a material exhibiting adequate gas tightness, good ion conductivity, a thermal expansion coefficient close to that of the electrodes (to prevent mechanical stress), further proof of being chemically inert with respect to the electrode materials, stability in both oxidizing and reducing environments and, finally, mechanical stability in high-temperature electrolysis operating conditions. The material that best satisfies these requirements and that is most used is the yttria-stabilized zirconia (YSZ). About the electrodes, the material selected must exhibit high electronic conductivity, together with high porosity to permit water and carbon dioxide diffusion in the SOEC mode, but also to allow the removal of hydrogen and carbon monoxide at the cathode and oxygen at the anode. For the cathode, the material is a cermet, generally a nickel/yttria-stabilized zirconia (Ni/YSZ) cermet. For the oxygen electrode, it is normally considered the reference compound the strontium-doped lanthanum manganite (LSM), and it is particularly suitable for operations above 800 °C [4].

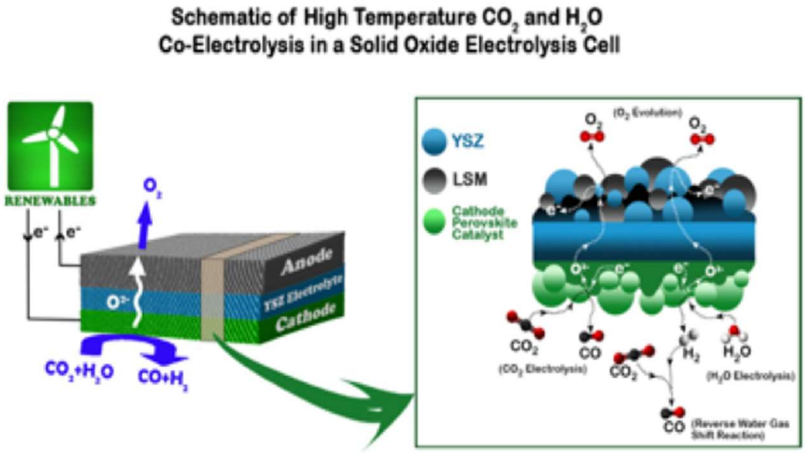

Figure 2. *Schematic of H_2O and CO_2 co-electrolysis in a SOEC* [13]

The high-temperature electrolysis used in our specific case is more advantageous than low-temperature proton exchange membrane (PEM) electrolysis and alkaline electrolyzers because SOEC can produce hydrogen at a higher chemical reaction rate with a lower electrical energy requirement and reduces the need for expensive catalysts [14]. In fact, working at a higher temperature results in the possibility of providing more energy in the form of heat instead of electricity.

2.1 Thermodynamics of High-Temperature Electrolysis

Considering a generic reacting system with the exchange of heat and electrical power, and with inlet and outlet material flows, under the following hypothesis:

- reversibility (ideal case);
- steady-state conditions.

It is possible to express, respectively, First and Second Law of Thermodynamics (for open systems) as follows [15]:

$$\Phi - W_{el}^{rev} = \sum \pm n_i \cdot h_i(T, p_i) \tag{1}$$

$$\frac{\Phi}{T} = \sum \pm n_i \cdot s_i(T, p_i) \tag{2}$$

Where n is the mole flow, h is the mole enthalpy, s is the mole entropy, Φ is the heat flux, W_{el}^{rev} is electric power in reversible conditions, T and p are respectively operative temperature and pressure. Sign "+" is assigned to outlet flows, sign "- "to inlet flows.

The previous equations change in the following by referring all the terms to the inlet mole flow n_{in}:

$$q - l_{el}^{rev} = \sum \pm v_i \cdot h_i(T, p_i) \quad \textbf{(3)}$$

$$\frac{q}{T} = \sum \pm v_i \cdot s_i(T, p_i) \quad \textbf{(4)}$$

Stoichiometric coefficient $v_i = n_i/n_{in}$ represents the ratio between a generic *i-th* mole flow and the inlet mole flow. Considering the following relations:

$$\sum \pm v_i \cdot h_i(T, p_i) = \Delta h \left[\frac{kJ}{kmol}\right] \quad \textbf{(5)}$$

$$\sum \pm v_i \cdot s_i(T, p_i) = \Delta s \left[\frac{kJ}{kmol}\right] \quad \textbf{(6)}$$

Substituting (5) and (6) respectively in (3) and (4) and remembering that Gibbs Free Energy g is $g = h - T*s$ it is finally obtained:

$$l_{el}^{rev} = -\Delta g \quad \textbf{(7)}$$

The equation (7) provides the electrical work in reversible conditions.

The only way to operate in reversible condition is the ideal condition of "open circuit" i.e., the condition in which there is no current flow in the external circuit. In fact, when the circuit is closed and there is charge moving through it, irreversible phenomena occur.

In order to finally derive the Nernst equation, is useful to mention the Faraday Law:

$$n_R = \frac{j \cdot A}{n_e \cdot F} \quad \textbf{(8)}$$

Where:

- n_R [mol/s] is the fraction of reactant mole flow which effectively reacts;
- j [A/cm^2] is the current density. Normally it is much used the concept of current density rather than the current itself, because the first gives a better description of cell performance and operating condition due to its size-independent feature;
- A [cm^2] is the active area of the cell;
- n_e is the number of electrons involved in an electrochemical reaction, namely released during oxidation or consumed during reduction;
- F is Faraday constant, and has a fixed value of 96,487 C/mol.

That said, electrical work in reversible conditions can also be written as:

$$l_{el}^{rev} = \frac{W_{el}^{rev}}{n_R} = \frac{I \cdot E}{\frac{I}{n_e \cdot F}} = n_e \cdot F \cdot E \quad \textbf{(9)}$$

Where E is voltage in reversible conditions, i.e., at open circuit.

So finally, the Nernst equation in a generic case is given by:

$$E = -\frac{\Delta g}{n_e \cdot F} \quad \textbf{(10)}$$

As said before E is the so-called open circuit voltage or otherwise reversible voltage; so, when the circuit is closed, irreversibility is generated; this means a voltage increase in the SOEC. The behavior of operative voltage as a function of the current density is expressed by the "Polarization Curve".

Irreversibility phenomena are conventionally grouped into three categories, each of those causes a voltage increase in the SOEC, so they are called overvoltages. The analytical expression of the polarization curve is the following:

$$V_{op}(j) = E + \eta_{act}(j) + \eta_{ohm}(j) + \eta_{diff}(j) \quad \textbf{(11)}$$

Where:

- η_{act} is the "Activation Overvoltage", due to the charge transfer from molecule to the electrode (in case of oxidation) or from the electrode to molecule (in case of reduction);
- η_{Ohm} is the "Ohmic Overvoltage", due to the ohmic losses arose in the cell because of the resistance opposed by the materials to the movement of electric charges (electrons and ions);
- η_{diff} is the "Diffusion (or Concentration) Overvoltage", to consider the fact that in the proximity of the reacting sites the concentration of reactants differs from the concentration that is considered calculating the open circuit voltage, due to diffusion phenomena.

The angular coefficient of the polarization curve is a parameter called "Area Specific Resistance" (ASR):

$$ASR = \frac{V_{op} - V_G}{j} \tag{12}$$

Where:

- V_{op} [V] is the operative voltage;
- V_G [V] is the reversible voltage;
- j [A/cm^2] is the current density.

The thermo-neutral voltage can be defined as the particular operative voltage at which the global heat flux is equal to 0: so, in this case, the heat generated by irreversibilities equals the heat required by the endothermicity of the reaction. It can be derived from the application of the First Law and considering the heat flux equal to 0:

$$q - l_{el} = \Delta h \tag{13}$$

$$V_{tn} = \frac{l_{el}(q = 0)}{n_e \cdot F} = \frac{\Delta h}{n_e \cdot F} \tag{14}$$

The thermo-neutral voltage is useful to define the efficiency of the cell:

$$\eta_{SOEC} = \frac{V_{tn}}{V_{op}} \quad \textbf{(15)}$$

The efficiency definition does not take into account the thermal input, but only refers to an electrical one. For this reason, η_{SOEC} can assume values larger than 1.

- Operating at voltages lower than the thermo-neutral one means that there will be good efficiency of the electrical part, but there will be the necessity of heat injection;
- Operating at voltages higher than thermoneutral one means that the cell will suffer from low efficiency.

The best trade-off between efficiency and plant complexity results to operate at the thermo-neutral condition, thus achieving the highest efficiency [16].

2.2 Simple electrolysis and co-electrolysis

The reaction of dissociation of the water is:

$$H_2O(l) \rightarrow H_2(g) + \frac{1}{2}O_2(g) \qquad \Delta H^0_{298\,K} = 286\ \text{kJ/mol}\ [4] \qquad \textbf{(16)}$$

In standard conditions of temperature and pressure (T=298 K, p=1 bar), water is liquid, and H_2 and O_2 are gaseous. It can be seen that enthalpy for water splitting also includes the vaporization heat, because, as stated before, in standard conditions water is at liquid state. Moreover thermodynamics, according to the value of the Gibbs Free Energy (ΔG_d=+237.22 kJ/mol), states that the water-splitting reaction is a non-spontaneous one. In acidic media, water splitting occurs according to:

$$H_2O(l) \rightarrow \frac{1}{2}O_2(g) + 2H^+ + 2e^- \qquad \textbf{(17)}$$

$$2H^+ + 2e^- \rightarrow H_2(g) \qquad \textbf{(18)}$$

These two reactions put together return the global reaction on equation (16).

In figure 3 the typical layout of a SOEC for steam electrolysis is showed.

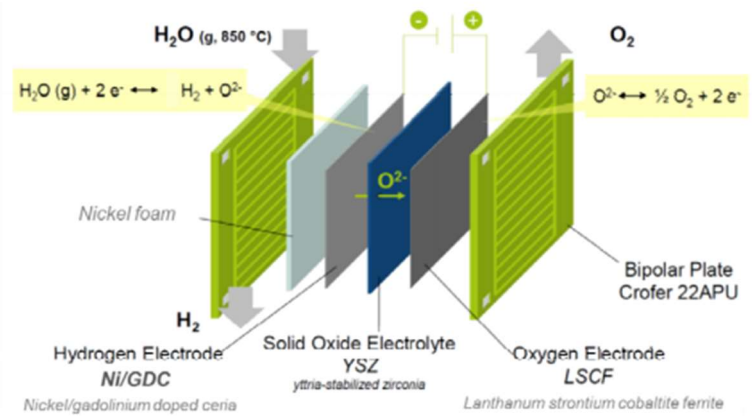

Figure 3. *Typical layout of a SOEC for steam electrolysis [17]*

The global reaction that occurs in the cell in the case of co-electrolysis of both water and carbon dioxide is:

$$H_2O + CO_2 \rightarrow H_2 + CO + O_2 \quad \textbf{(19)}$$

So, the carbon dioxide and water together flow into SOEC cathode and both take the electrons from the external electric source to split in CO, H_2 and O^{2-} ions on the cathode; these last are transported through the electrolyte layer and then evolve as O_2 on the anode.

The global reaction can be further separated into two electrochemical reactions:

$$H_2O + 2e^- \rightarrow H_2 + \frac{1}{2}O_2 \quad \textbf{(20)}$$

$$CO_2 + 2e^- \rightarrow CO + \frac{1}{2}O_2 \quad \textbf{(21)}$$

2.3 Operational conditions

As said before, with increasing the operating temperature the total energy demand remains unchanged while the electric demand drops and heat demand grows and figure 4 (referred to the co-electrolysis case) gives a graphical representation of it. Being the heat sources often available at lower prices than the electric ones, this results in high efficiencies of the cell as well as a reduction of the cost of production.

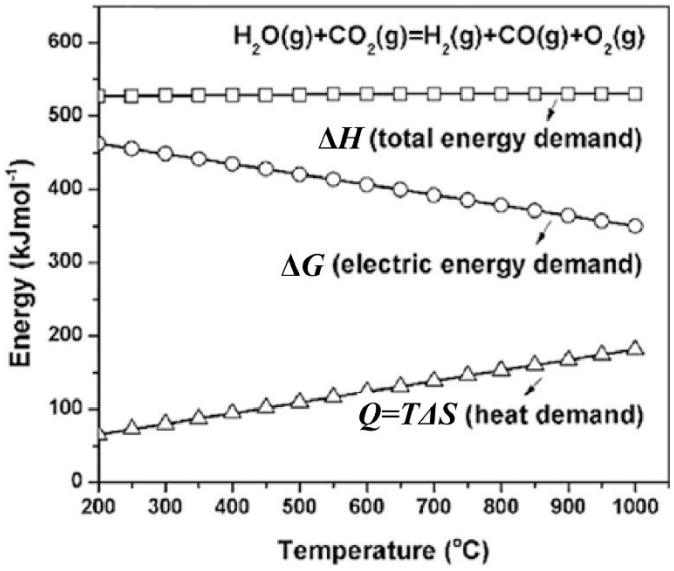

Figure 4. *Energy demanded as a function of the temperature for the co-electrolysis process* [18]

High temperature electrolyte cells can operate near 100% electricity-to-fuel efficiency [19].

The pressure at which the SOEC is operated is also a key factor, and it is possible to find an optimal value between the electrolyzer system and the reactors for syngas conversion. It has been reported that by pressurizing the SOEC stack, the PTG efficiency will increase by 3÷4% [20]. By working in pressure would also result in an improvement of the performance of the SOEC: it has been reported that for hydrogen production in cathode supported cell the pressurization resulted in an enhanced performance of the SOEC at electrolysis current densities above 0.5 A/cm^2 [14]. In fact, increasing pressure can bring to an increase in gas diffusion rates and it can also be the possibility of methane formation directly on the cathode for the presence of Ni and high pressure.

2.4 Parameter influencing the SOEC output

The main parameters that affect the output of SOEC are operating temperature, pressure, inlet gas composition and reactant utilization and these have been studied in the work of Sun et al. [19] considering a system for the production of methane.

2.4.1 Temperature

As we said before, an increase of temperature will lead to less electric energy consumptions and then better efficiencies of the cell itself; nevertheless there are other parameters that have to be taken into account, and the most important is component degradation: in fact lower temperatures cause slower kinetics and worse efficiencies but allows the subsistence of optimized microstructures and nanoparticles (which promote faster kinetics) against sintering and agglomeration, thus balancing out the cell performance.

Furthermore, considering the goal of the process the production of methane, lower temperatures coupled with high pressures will foster the formation of methane directly on the cathode (also thank to the Ni-based cathode which is usually used).

Considering the work of Sun et al. [19] the dependence of outlet gas composition with respect to temperature is reported in figure 5. This trend is reported considering a pressure of 35 atm and 70% reactant utilization with inlet gas molar composition 10% H_2, 25% CO_2, 65% H_2O.

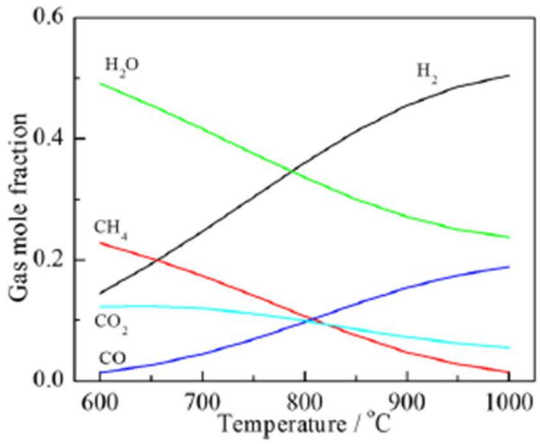

Figure 5. *Outlet gas composition wrt operation temperature of the SOEC* [19]

As it can be seen, decreasing the SOEC operating temperature from 1000 °C to 600 °C, the methane equilibrium concentration in the downstream gas products is increased from 1.5% to 22.8% confirming what was said before. However, the production of methane directly inside the SOEC and so the occurring of the reaction of methanation that is highly exothermic (it will be discussed in the following section) may create a marked temperature gradient across the cells, so the thermal management of it becomes a tricky issue.

2.4.2 Pressure

The role of pressure is fundamental because increasing the pressure will increase the reversible voltage of the stack but decrease the thermo-neutral voltage since more methane will be formed [21].

In figure 6 the dependence of the outlet molar composition with respect to the pressure in the stack is showed, having fixed fuel utilization to 70% temperature to 850 °C and inlet gas composition at 10% H_2, 25% CO_2, 65% H_2O.

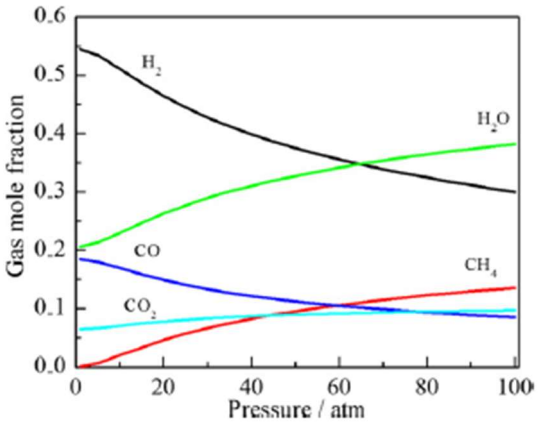

Figure 6. *Outlet gas composition wrt operation pressure of the SOEC* [19]

With increasing pressure, the molar fraction of H_2O and CH_4 and slightly of CO_2 increase, but that of H_2 decreases as well as that of CO.

2.4.3 Reactant Utilization

The reactant utilization (RU) is defined in equation (22):

$$RU = \frac{\dot{n}_{react,in} - \dot{n}_{react,out}}{\dot{n}_{react,in}} \quad \textbf{(22)}$$

In which $\dot{n}_{react,in}$ and $\dot{n}_{react,out}$ are respectively the inlet and outler molar flows, expressed in mol/sec.

Figure 7 shows the dependence of the outlet molar composition with respect to the reactant utilization. At a temperature of 850 °C and pressure of 35 atm, increasing the fuel utilization will result in a drop of H_2O and CO_2 molar fraction but more production of CH_4 and H_2. Regarding the CO it is possible to see that it has a maximum in correspondence of RU=70% and above it, its molar fraction decreases.

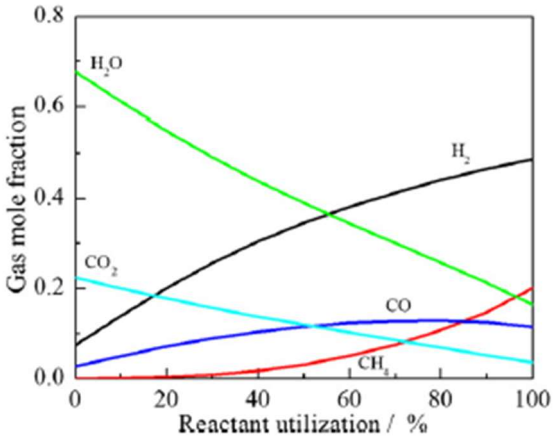

Figure 7. *Effect of reactant utilization on outlet gas composition* [19]

3. Overview on methanation

Methanation processes are procedures whose purpose is that of producing synthetic natural gas from a mixture of hydrogen and carbon dioxides, i.e., syngas. The conversion of carbon monoxide is referred to as CO methanation, while the conversion of carbon dioxide as CO_2 methanation respectively.

3.1 Principles of methanation

The main reactions occurring during a methanation process are the CO methanation (eq. (23)), CO_2 methanation (eq. (24)), and water gas shift (eq. (25)):

$$CO + 3H_2 \rightarrow CH_4 + H_2O \qquad \Delta H^0_{298\,K} = -206\ \text{kJ/mol}\ [22] \qquad \textbf{(23)}$$

$$CO_2 + 4H_2 \rightarrow CH_4 + 2H_2O \qquad \Delta H^0_{298\,K} = -164\ \text{kJ/mol}\ [22] \qquad \textbf{(24)}$$

$$CO + H_2O \rightarrow CO_2 + H_2 \qquad \Delta H^0_{298\,K} = -41\ \text{kJ/mol}\ [22] \qquad \textbf{(25)}$$

Water gas shift conversion is a reaction that always occurs simultaneously to the other two in the presence of active catalysts. It has been observed that the whole transformation of carbon dioxide into methane starts with a reverse shift conversion reaction with hydrogen to obtain steam and carbon monoxide which is subsequently transformed into methane.

Performing the methanation process from a plant point of view may result in heat issues: in fact, the methanation reaction is highly exothermic one, and it is favoured not only at lower temperatures but even at high pressures; those high pressures involve large amounts of heat produced per volume compared to low-pressure processes, so the heat management and removal are essential in order to avoid the compromising of the methane yield or of the catalyst, necessary for the kinetics of the reaction.

The methanation reactor technologies may be subdivided into three main categories: fixed bed, fluidized bed and other. In the following section, the attention will be focused about the TREMP™ (Topsøe Recycle Energy-efficient Methanation Process)

process [23], that is the model from which the methanation part of this work has been modeled by.

3.2 Overview on TREMP™ process

Figure 8 shows a summary diagram of the various blocks of which the SNG plant is composed. The feedstock is initially gasified in the presence of O_2 and H_2O. The gas is then cooled and cleaned for tars, salts and dust. The ratio between H_2 and CO is adjusted in the sour shift by the water gas shift reaction. The syngas coming from the sour shift is rich in sulphur (H_2S) and CO_2. Being the sulphur an inhibitor for the methanation catalyst and in any case unwanted in the product, it must be removed. The CO_2, as well, has to be removed in order to reach the right hydrogen to carbon ratio, which will be described afterward.

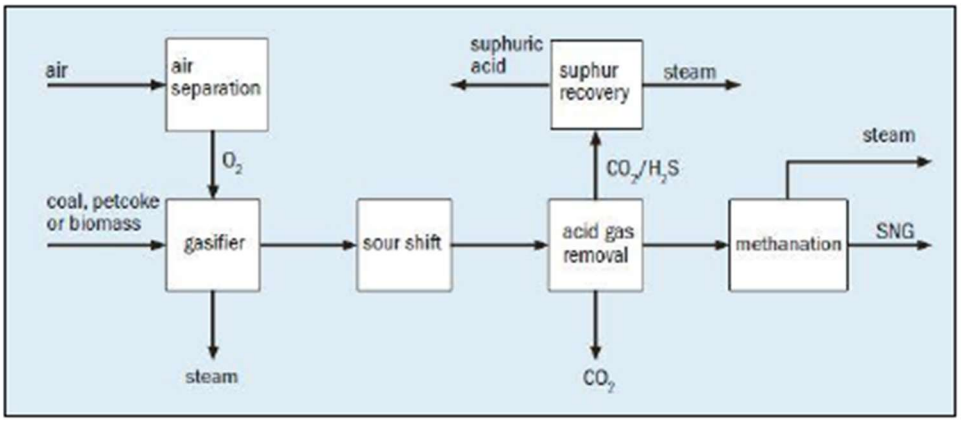

Figure 8. *Block diagram of the TREMP™ process* [24]

The syngas exiting the sour shift is then treated in the acid gas removal (AGR) unit, where the removal of H_2S and CO_2 occurs. CO_2 from the AGR can be sequestrated or used for other purposes, and H_2S can be furtherly treated to obtain sulphuric acid, which is a high-value product in many regions.

The treated gas is then sent to the methanation block.

3.2.1 Methanation block overview

As seen in previous sections both CO and CO_2 methanation reactions are strongly exothermic ones. So, if syngas with a minimum methane level is introduced into an

adiabatic methanation reactor at 300 °C, the resulting exit temperature will be around 900 °C [2]. This thing causes issues with the material selection and insufficient catalyst activity because it would take a high-temperature stable catalyst with also a high activity at low temperatures. A solution to this problem may be the diluting of inlet gas through recirculation in order to keep the temperature below 450 °C; however, being the first step of methanation in need of compression and increased volumetric flow, this results in higher costs of compression, both in terms of electrical power and maintenance.

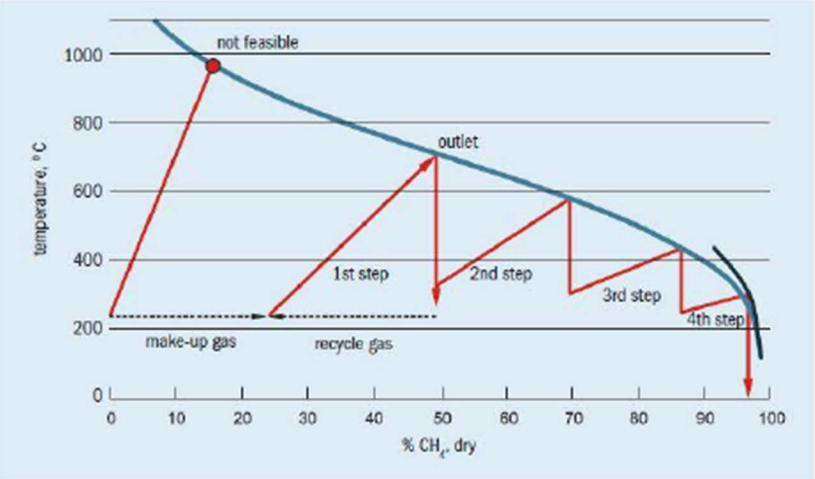

Figure 9. *Equilibrium Curve for methanation process for a specific pressure* [23]

The solution at all this problem, in order to obtain at the end of the methanation step a product with more than 95% of methane, the methanation process has to be performed in more step, so more adiabatic reactors working at decreasing temperature levels and split by intermediate cooling. The exact number of reactors is chosen considering a trade-off between requirements of product gas quality and heat recovery.

In particular, as regards to TREMP™ technology, a schematic of the methanation section is shown in figure 10. The strength of this technology is the conjugation of minimum recycle cost and heat recovery in a very efficient way.

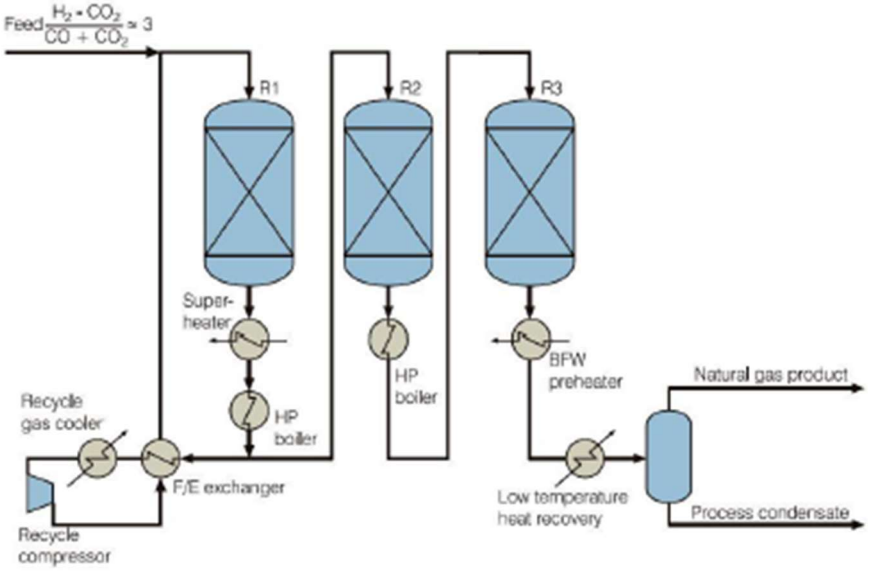

Figure 10. *Scheme of TREMP™ methanation process* [24]

The subsequent operations included in this block are the following: the feeding gas first passes through a sulphur guard bed for removal of traces of sulphur that have not been removed over the AGR; the desulphurized feed is then sent to the first methanation reactor but before it is mixed with recycle gas to control the temperature. After the first methanation stage, the reaction heat is recovered and used for the generation of superheated high-pressure steam in the downstream heat exchangers (this is what occurs in the layout of figure 10, but the heat recovered could also be used for thermal integration of the whole plant). Then there are other additional methanation reactors whose number depends on sundry factors, such as pressure, but also the technical requirements of the final product. If the number of the reactors is more than four, there is also the possibility of an additional operation before the last methanation step, that is the removal of water generated in the previous methanation steps so that the equilibrium will be shifted further towards methane formation. After this the SNG obtained is subject to completion operations such as cooling, drying, compressing and eventually correction in order to fulfill the technical specifications of the admission in the grid.

4. Process models description

In this chapter is reported the description of the models used for the modeling of the plants for the production of methane and hydrogen. The program used to develop the plant layouts and through which have been performed the simulations to achieve all the useful data for this work has been Aspen Plus™.

The first model has the purpose of simulating a system based on co-electrolysis coupled with methanation to produce methane, the second is almost equal to the first except for the fact that at the inlet of the SOEC there is already a mixture of water and syngas from gasified biomass, while the third and last provides a simulation of only steam electrolysis to produce hydrogen.

The main hypotheses and assumptions made in the case of co-electrolysis and methanation are summarized in table 1 [2]:

Table 1. *Hypotheses and assumptions for co-electrolysis+methanation*

Stack Pressure [bar]	Stack Temperature [°C]	[H_2] at cathode inlet	Reactant Utilization (RU)	Methanators inlet temperature [°C]
33.1	850	10%	70%	220

In table 2 the main hypotheses and assumptions made in the case of steam electrolysis are stated [25]:

Table 2. *Hypotheses and assumptions for steam electrolysis*

Stack Pressure [bar]	Stack Temperature [°C]	[H_2] at cathode inlet	Reactant Utilization (RU)
60	850	10%	70%

It is assumed that in all configurations the voltage at which the SOEC is operated is the thermo-neutral voltage, for the reasons explained in section 2.1. In table 3 the values of thermo-neutral voltages used in each simulation are listed.

Table 3. *Values of thermo-neutral voltage for each configuration*

SNG production from CO_2 [V]	**SNG production from gasified biomass [V]**	**H_2 production [V]**
1.2228	1.1133	1.6094

4.1 Co-Electrolysis + Methanation

4.1.1 Electrolysis section

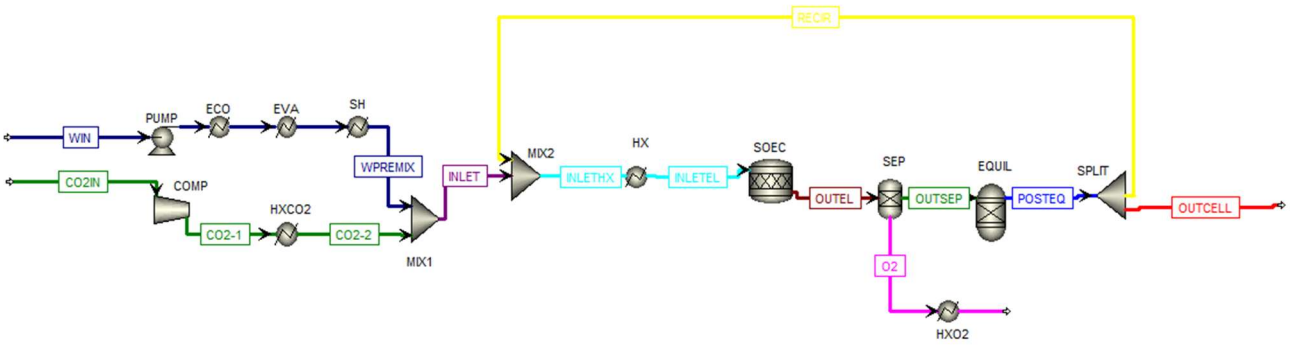

Figure 11. *Co-Electrolysis model on Aspen Plus™*

A brief description of the main components in co-electrolysis block is given. The model here described was in principle developed by Giglio et al. [2].

PUMP is the component in which water pressure is increased both to compensate pressure drop during following evaporation and because it has been chosen to make work the SOEC in pressure. Although this choice may not necessarily give advantages from an electrochemical point of view, is good in the global energy economy of the system: in fact, is much more convenient not to compress the gaseous syngas produced after the SOEC (which moreover will also be at higher temperature, involving more compression work), but rather to pump liquid water before SOEC inlet. As said in section 2.4.2 carrying out the electrolysis at higher pressures also allows to generate methane already at the cathode, that is a great advantage because less methane has to be produced during methanation, less heat has to be removed during methanation reaction thus allowing the reduction of the number of reactors. Pressure drop during evaporation of water has been set as 10% of total pressure, according to [26].

ECO, *EVA* and *SH* are three heaters in which pre-heating, evaporation and superheating of water are realized.

COMP and HXCO2 are respectively a compressor and a heater used to bring the entering carbon dioxide to the operating condition (temperature and pressure) of the cell.

MIX2 and *SPLIT* are respectively a mixer and a splitter. They realize a recirculation of the syngas to ensure a minimum concentration of H_2 at the cathode inlet. This is done to avoid a too-oxidant atmosphere at the cathode side, in which Ni is present as a catalyst. Ni oxidation would represent a problem both for catalysis of the electrode and for cell structural strength. This fraction of hydrogen was set equal to 10% mole according to [27].

HX, *SOEC*, *SEP* and *EQUIL* simulate the co-electrolysis process. *HX* is a heater that simply restores the operative temperature of the cell that is altered (slightly decreased) because of the recirculation. In real plant this can be accomplished by working at a voltage slightly higher than thermoneutral voltage.

SOEC is a stoichiometric reactor. It requires the knowledge about reactant, products and fractional conversion [28]. For it these two reactions are specified:

$$2H_2O \rightarrow 2H_2 + O_2 \quad \textbf{(26)}$$

$$2CO_2 \rightarrow 2CO + O_2 \quad \textbf{(27)}$$

Obviously, this is not what actually occurs into an electrolysis cell. Aspen Plus™ has not a built-in component for the simulation of an electrochemical device: since no electrons are involved, what in a real device is expressed as an electrical input, in this model will be expressed as Heat Duty. This does not affect the numerical result of the simulation because the form through which energy is supplied changes, but its numerical value does not change. Stoichiometric reactor also requires the specification of fractional conversion of a key reactant (steam and carbon dioxide in this case). This value has been set at 70% [19].

EQUIL is a Gibbs reactor whose aim is to simulate all chemical reactions that may take place at the cathode side such as Water Gas Shift (WGS) and methanation of CO, as discussed in section 3.1.

SEP is a separator which effectively realizes the physical separation between the anode and the cathode side. In the anodic side of the cell only oxygen is produced, so in the component specifications are imposed a mechanical separation of the oxygen stream from the other substances.

HXO2 is the oxygen cooler, the outlet temperature is 35 °C and pressure drop was set to 0.7 bar.

The operation of the cell has been modeled to achieve an outlet syngas with the required feed ratio (FR) defined according to equation (28). The feed ratio depends on the desired synfuel quality, which depends on optimal conditions to maximize the subsequent synthesis reaction. In this specific case, FR has been set equal to 3 [2].

$$\frac{H_2 - CO_2}{CO + CO_2} = 3 \qquad \textbf{(28)}$$

Normally the feed ratio of the gas to the methanation unit is settled by adjusting the by-pass of the sour shift unit. By increasing the by-pass, less CO and water is converted into H_2 and CO_2 through the WGS reaction. This does not affect the FR directly, but, being the CO_2 removal rate in the AGR almost constant, the FR will decrease when the sour shift by-pass is increased. In this specific case, the FR is adjusted by modulating the flow rate of the inlet water. As figure 12 shows, at FR=3 the methane yield is maximum.

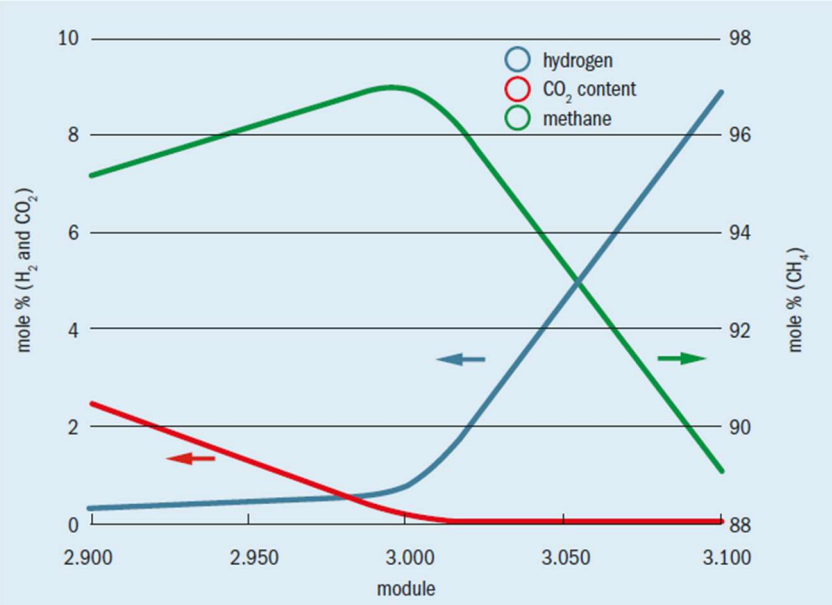

Figure 12. *SNG product quality wrt FR values*

It must also be said that the layout proposed in this work, i.e., electrolysis section + methanation section, allows achieving a simplification of the plant configuration of layout with respect to the one described in TREMP™ layout: in fact the coupling of electrolysis and methanation allows to exclude all the components that carry out the cleaning and the correction of the syngas, such as gasification, air separation, sour shift and AGR, if hypotheses of working with demineralized water and almost pure carbon dioxide are made.

The molar composition of the flow entering the SOEC after recirculation is represented in figure 13.

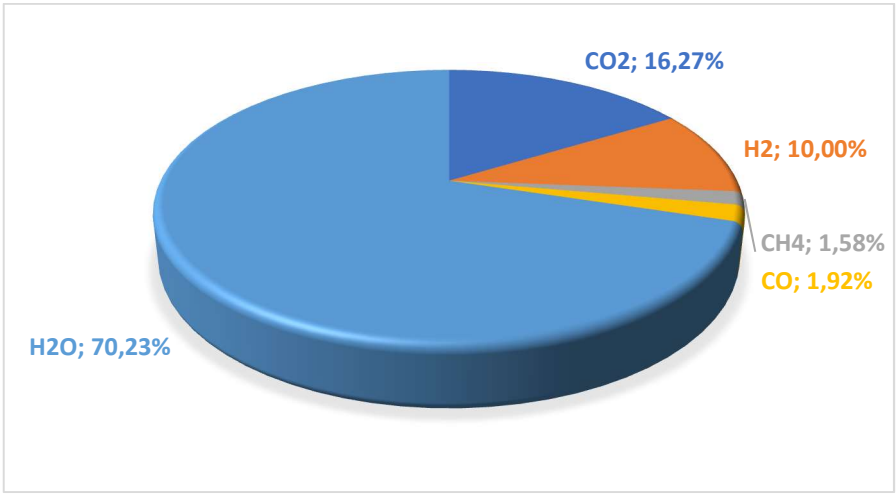

Figure 13. *SOEC inlet flow molar composition after recirculation*

The molar composition of the flow exiting the SOEC is represented in figure 14.

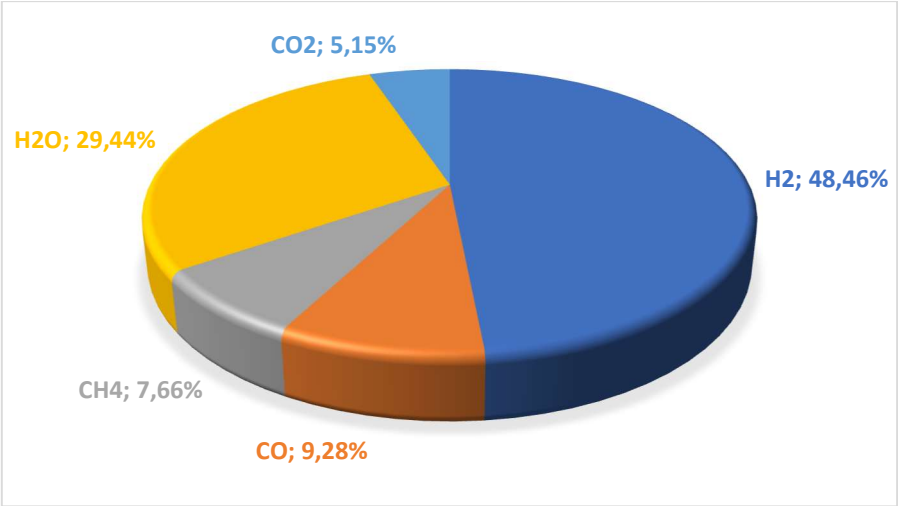

Figure 14. *SOEC outlet flow molar composition*

4.1.2 Methanation and cleaning section

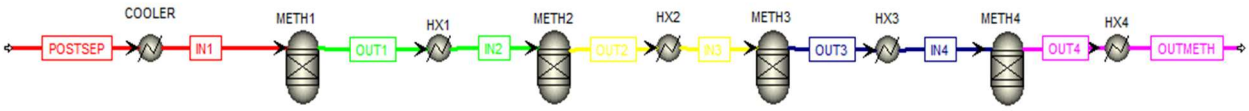

Figure 15. *Methanation model on Aspen Plus™*

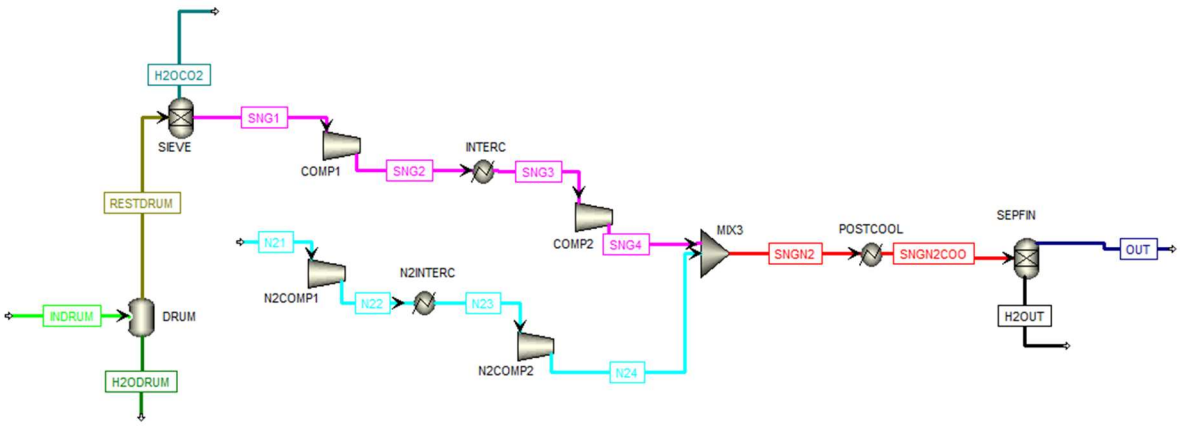

Figure 16. *Cleaning and correction section modeled on Aspen Plus™*

Concerning figure 15, below the single components are described.

COOLER is a heat exchanger for the syngas exiting the electrolysis section: this is done because of the different temperature between the electrolysis section and the

methanation section; this temperature was set 220°C [23] and the pressure drop was set 0.1 bar.

METH1, *METH2*, *METH3* and *METH4* are the reactors in which the methanation reaction occurs. In Aspen Plus™ these reactors are modeled as Gibbs reactor, i.e., a reactor that brings a mixture of chemical species to chemical equilibrium by minimizing the Gibbs Free Energy. Reactors are modelled as adiabatic [29] (the other opportunity is to model them as isothermal ones). Contrary to the TREMP™ plant, there is no recirculation in the first reactor, because it is not performed in it the carbon monoxide methanation but the carbon dioxide methanation which is less exothermic. This represents a huge advantage both in terms of methanation efficiency and plant efficiency (because for the recirculation it is necessary a recirculating compressor that consumes electric energy. The pressure drop of each methanator was set to 0.7 bar [29]. In table 4 the fraction of CO_2 converted in each step is reported.

Table 4. *Fraction of CO_2 converted in each methanation step*

Step 1	5.476 %
Step 2	59.603 %
Step 3	92.441 %
Step 4	97.914 %

HX1, *HX2*, *HX3* and *HX4* are intermediate coolers whose function is to refrigerate the outlet mixture from the previous methanator; this is done to further shift the equilibrium towards the formation of methane in the subsequent reactors. The outlet temperature of each cooler has been set to 220 °C, and the pressure drop has been set 0.7 bar [29].

In figure 17 the methanation section outlet flow molar composition is represented.

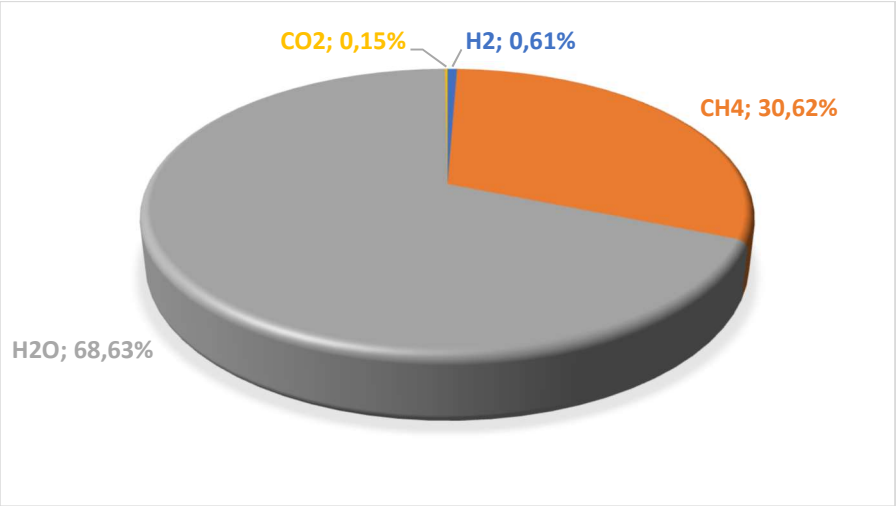

Figure 17. *Methanation section outlet flow molar composition*

With reference to figure 16, below the single components are described.

DRUM is a flash separator which allows the thermodynamic equilibrium between the liquid phase and the gaseous phase. The role of this component is to separate an extensive quantity of water from the raw mixture. This recovered water could also be recirculated at the inlet of the electrolysis section to have a positive impact both from the environmental point of view and the economic one.

SIEVE is a molecular sieve which furtherly refines the mixture exiting the methanation section. In particular, it retains substances like water and carbon dioxide (especially water is a product of both methanation reactions so present in high concentration and is also a not desirable element into a gas pipeline). The molecular sieve retains almost all the water and 98.5% of carbon dioxide [29].

COMP1, *INTERC* and *COMP2* are components of natural gas compression section, bringing gas pressure to a value of 60 bar, which is a typical value of natural gas pipeline pressure.

N2COMP1, *N2INTERC* and *N2COMP2* are component for nitrogen compression section. In fact, in order to fulfill the prescription for the admission in the grid, the SNG has to be furtherly corrected by this stream of nitrogen.

SEPFIN is a final membrane separator which is used to fulfill the prescription about the volume percentage of the hydrogen in the final product that is put in the grid.

Membrane separation is a technology which selectively separates (fractionates) materials via pores and/or minute gaps in the molecular arrangement of a continuous structure. Membrane separations are classified by pore size and by the separation driving force. These classifications are: Microfiltration (MF), Ultrafiltration (UF), Ion-Exchange (IE), and Reverse Osmosis (RO). The other way to obtain a higher purity of the outlet SNG is to use, instead of adiabatic reactors as done in this work, isothermal reactors, whose rate of conversion of carbon dioxide is much higher than adiabatic ones [30], thus decreasing the volume percentage of hydrogen in the final mixture; however, even with this solution, the prescribed volume percentage was not ensured.

In this case, the prescriptions established in Italy for pumping natural gas into pipelines have been used [31].

The main parameters that must be severely controlled are:

- Gas Gravity;
- Wobbe Index;
- Higher Heating Value of produced SNG.

Gas Gravity (eq. (29)) is the ratio between densities of produced SNG and air, both calculated in Standard Conditions, which are the pressure of 101,325 Pa and temperature of 288.15 K [32].

$$GG = \frac{\rho_{SNG}}{\rho_{air}} \quad \textbf{(29)}$$

Simplistically considering air being constituted only by oxygen and nitrogen, molar composition respectively of 21% and 79%, ρ_{air} was set to a value of 1.22 kg/Sm^3 having found a value of molar mass equal to 28.84 kg/kmol.

Wobbe Index is described by the equation (30):

$$WI = \frac{HHV}{\sqrt{GG}} \tag{30}$$

HHV is the Higher Heating Value of SNG.

In the definition of the HHV, only methane contribution was prudently considered, not considering the contribution of the hydrogen, which is itself a fuel, but is also present in minimum quantity in the final mixture.

The ranges prescribed for each parameter by [31] are summarized in table 5.

Table 5. *Acceptability boundaries which allow SNG input in pipelines*

HHV [MJ/Sm³]	34.95÷45.28
Wobbe Index [MJ/sm³]	47.31÷52.33
Gas Gravity	0.5548÷0.8

There are also other prescriptions regarding natural gas molar composition, summarized in table 6 [31].

Table 6. *Limitations on the composition of SNG*

Carbon Monoxide (CO) [% mol]	≤0.1
Silicon (Si) [ppm]	≤5
Ammonia (NH_3) [mg/Sm³]	≤3
Hydrogen (H_2) [% vol.]	≤0.5
Mercury (Hg) [µg/Sm³]	≤1
Fluorine (F) [mg/Sm³]	<3
Chlorine (Cl) [mg/Sm³]	<1

It has been verified that the SNG had to be mixed with the nitrogen because of too low gas gravity. This is explicable considering that SNG is essentially composed of methane and hydrogen, so it is too "light".

From a simulation point of view, the target has been achieved using a design specification, imposing a target value of GG equal to 0.555, varying nitrogen flow.

In figure 18 the final outlet flow molar composition is showed.

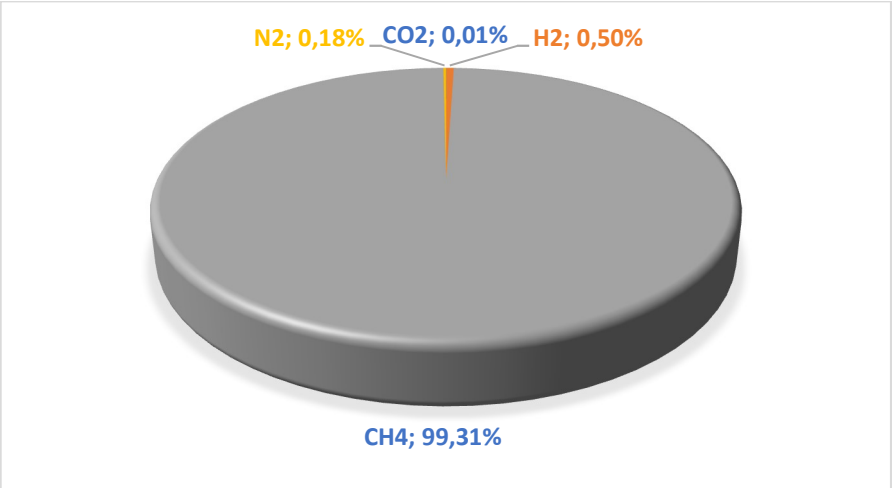

Figure 18. *Final outlet flow molar composition*

4.2 Co-Electrolysis + Methanation for syngas from biomass gasification

In the case of upgrading syngas derived from biomass gasification, the layout of the whole co-electrolysis and methanation section is almost the same as the previous section except by two things:

- there is no more recirculation from the outlet of the SOEC to the inlet cathode; in fact, this expedient has been used, as previously said, in order to ensure a fixed fraction of hydrogen at the inlet cathode, in our case equal to 10%. In this specific case the composition of the syngas entering the SOEC (even when mixed to the water to ensure the FR target) is already rich in hydrogen, so the presence of recirculation is no more needed;
- there is no more the correction part with the nitrogen; in fact, being the nitrogen already present in the initial syngas, this has resulted in total

fulfillment of the prescription of the admission into the grid even without additional nitrogen.

All other components and operations are equal to the previous case. In figure 19 the composition of syngas from biomass gasification is shown. This one has been chosen as the one reported by [33].

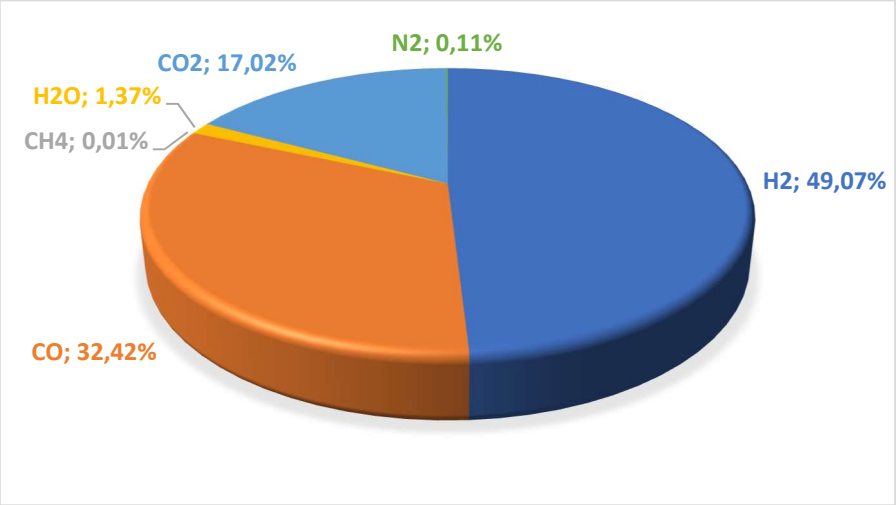

Figure 19. *Syngas from biomass gasification molar composition* [33]

4.3 Steam Electrolysis

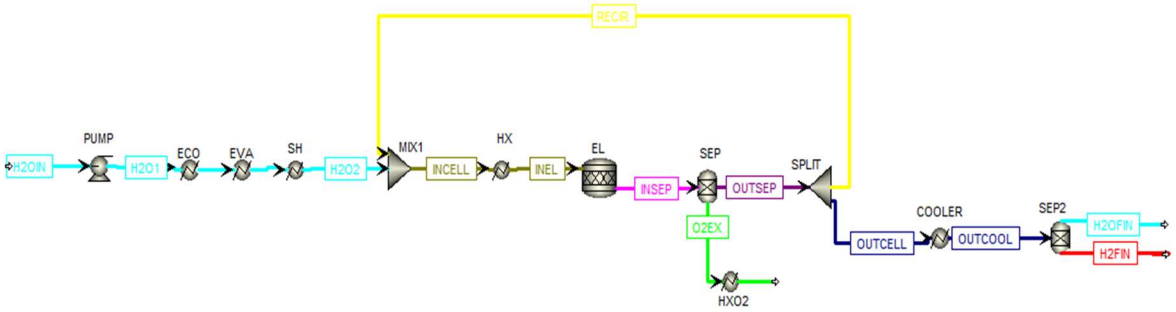

Figure 20. *Steam Electrolysis model on Aspen Plus™*

In figure 20 the scheme of the steam electrolysis layout is represented.

The layout is equal to the scheme previously showed, but in this case, since the goal is the hydrogen production and not the SNG production, the methanation section is not present. In this case, the electrolysis is driven at 60 bar: the choice of this pressure has been made considering parallelism with the typical value of natural gas pipeline pressure, although it is not yet present an infrastructure for the hydrogen distribution as a fuel. The choice of pumping the water before the cell and not to compress the gas exiting the cell can be understood by the fact that is much more convenient, from an energy expenditure point of view, increasing the pressure of a liquid rather than to compress a gas. So, this solution leads to energetic and also electrochemical advantages [34] [12].

5. Method

In this section, the method used to perform the feasibility analysis for the substitution of the natural gas in the industrial sector with synthetic ones (H_2 and SNG) is described. First, the consumption of natural gas in the industrial sector on a regional scale for the year 2018 has been computed starting from the historical data available until 2016. Then all the data related to the availability of the necessary resources have been collected; most of them are not related to 2018 but to previous years because of the limited availability of data from different sources; however, through the analysis of the historical data (which anyway were not available for all years), a significant modification of the order of magnitude of the data itself has not been seen, so it has been considered reasonable to use them.

Each region has been considered as an independent entity regarding demand and readiness of the necessary resources; this has been done to keep the analysis coherent at the local scale, hence allowing to perform also a comparison among the regions. Furthermore, the analysis performed has been done only from a quantitative point of view: namely it has been considered a hypothetical plant, unique for each region, based on the models shown previously; this has been done in order to study the feasibility only from a resources availability point of view, thus not facing other issues that can arise by the effective realization of the project.

Finally, the different synthesis routes are summarized.

5.1 Demand analysis of natural gas for the industrial sector in Italy

An analysis of historical data series on regional base has been performed to forecast the demand for the year 2018. The historical data of consumption of natural gas for the industrial sector has been provided by "*SNAM Rete Gas, S.G.I. s.p.a.*" processed by the Italian Minister of the Economic Development (MSE) [35]. However, from this source the data for region Sardinia were not provided, so the analysis for it has not been performed. In figure 21 the average consumption of natural gas on a regional scale in the time frame 2002-2016 is shown.

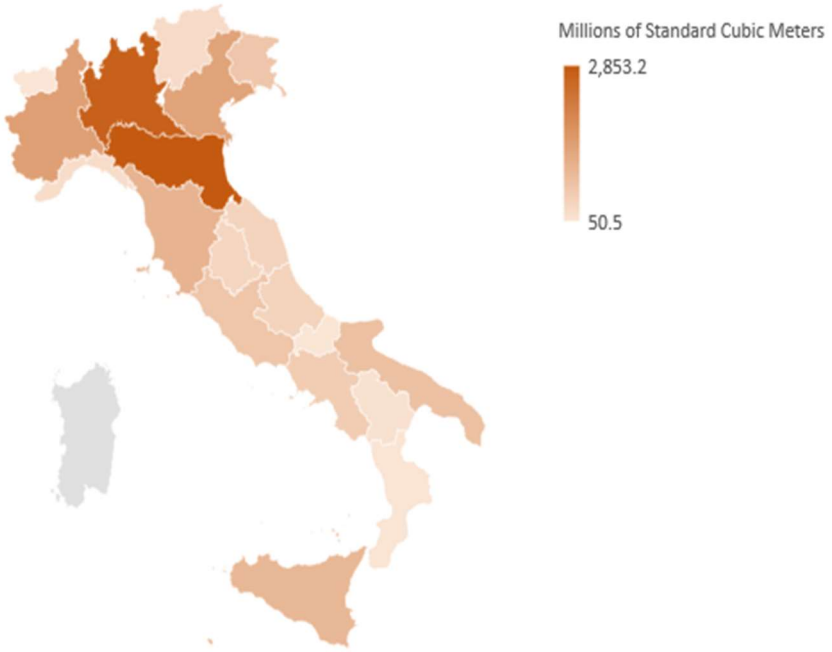

Figure 21. *Average consumption of natural gas on a regional scale in the time frame 2002-2016*

From the map of figure 22, it can be seen that most of the demand is by the northern regions of Italy.

The Holt Method [36] has been used to produce a short-term forecast of the gas consumption using historical data in time frame 2002-2016. This method is one of the exponential smoothing method, in particular it is a double exponential smoothing method: this name is due to the fact that simple exponential smoothing does not act well when there is a trend in the data, problem that is solved by the introduction of a term in the equations of the original method able to take into account the possibility

of a series exhibiting some form of trend. Furthermore, Holt Method is suitable for series with a trend but with no seasonality.

Starting from the historical series of gas demand it is possible to identify the trend in demand; the forecast *(P)* for the *(n+k)* year is then obtained using the trend *(T)* and the data's smoothed value *(S)* (eq. (31)). To evaluate the trend and the smoothed value at time *n*, the previous *n-1* data are used considering two different smoothing factor: the data smoothing factor (*a*) (eq. (32)) and the trend smoothing factor (β) (eq. (33)).

$$P_{n+k} = S_n + T_n \cdot k \tag{31}$$

$$S_n = \alpha \cdot d_n + (1 - \alpha) \cdot (S_{n-1} + T_{n-1}) \tag{32}$$

$$T_n = \beta \cdot (S_n - S_{n-1}) + (1 - \beta) \cdot T_n \tag{33}$$

In equation (30) d_n is the data for the industrial sector consumption at time *n*. The two smoothing parameters can vary between 0 and 1 and have been computed through a Matlab® script in order to minimize the root mean square error (RMSE) defined in equation (34). The optimization of the two parameters consents to simulate the behavior of the demand and thus to accomplish short-term forecasts. The method must be initialized, and it is achieved through the equations (35) and (36): the initial smoothed value is taken equal to the first data value, and the initial trend value is chosen as the difference between the second and the first data values.

$$RMSE = \sqrt{\left(\sum_{i=1}^{n} \frac{(P_i - d_i)^2}{n}\right)} \tag{34}$$

$$S_1 = d_1 \tag{35}$$

$$T_1 = d_2 - d_1 \tag{36}$$

In figure 22 the example of 2018 forecast for region Piemonte is shown, while in figure 23 the percentage error between model and effective data for the same region is shown.

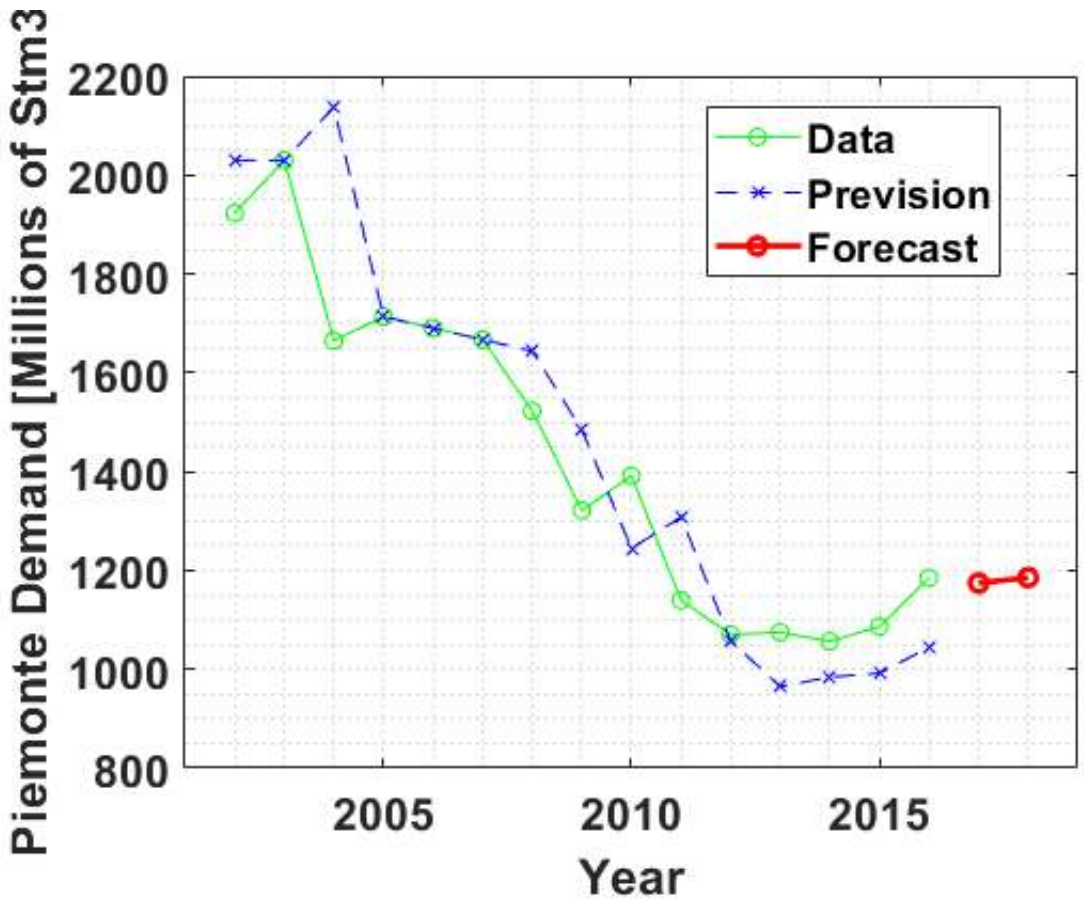

Figure 22. *Forecast for region Piedmont of gas consumption for years 2017-2018*

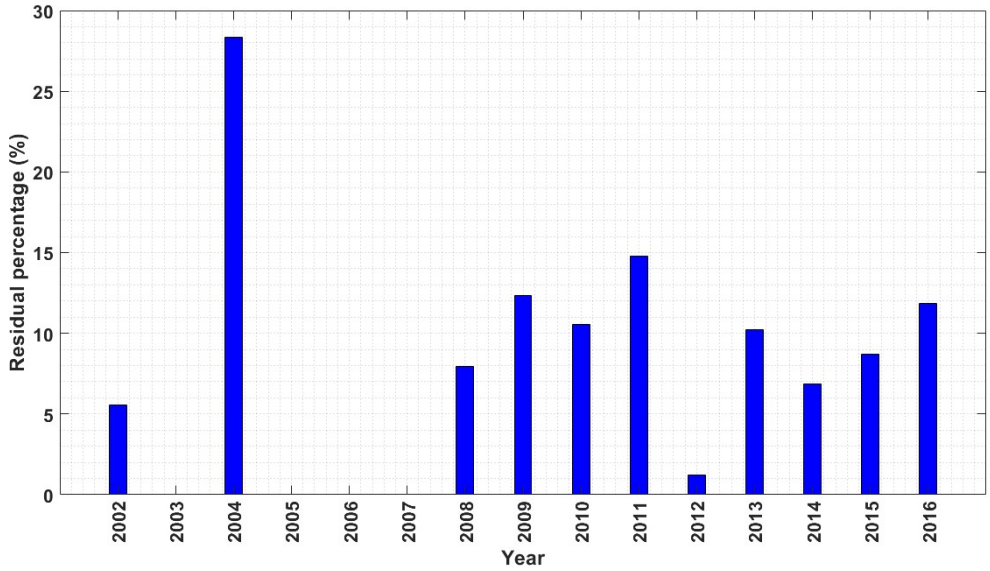

Figure 23. *Percentage error between real data and prevision among the years for region Piedmont*

In table 7 the forecast for years 2017 and 2018 and the energy demand for 2018 considering 38.1 MJ/Sm^3 as LHV of natural gas [35].

Table 7. *Forecasts for natural gas consumption in the industrial sector*

Region	2017 Forecast [Million of Stm^3]	2018 Forecast [Million of Stm^3]	2018 Energy Demand [PJ/year]
Piedmont	1,174	1,186	45.17
Aosta Valley	47	46	1.76
Lombardy	2,591	2,606	99.27
Trentino-S. T.	316	327	12.47
Veneto	1,399	1,443	54.96
Friuli V. Giulia	586	590	22.49
Liguria	143	117	4.46
Emilia Romagna	2,708	2,750	104.79
Tuscany	893	880	33.53
Umbria	258	249	9.50
Marche	362	358	13.63
Lazio	607	616	23.45
Abruzzo	327	329	12.54
Molise	17	20	0.75
Campania	454	447	17.02
Apulia	851	865	32.96
Basilicata	166	179	6.83
Calabria	43	41	1.55
Sicily	854	831	31.67
Sardinia	/	/	/
ITALY	*13,797*	*13,879*	*528.80*

5.2 Resources availability for the production of the fuels

In the analysis the following material and energy sources will be considered for the H_2 and SNG production:

- residual biomass as a source of syngas (a mixture of CO and H_2);
- CO_2 as a source of CO;
- H_2O as a source of H_2;
- electricity from V-RES to drive the electrolysis plant, the auxiliary parts and the processes for syngas recovering and carbon capture technology.

5.2.1 Residual Biomass

The availability of biomass at the regional level has been considered through a study made by ENAMA (Italian Institution for Agricultural Mechanization) in 2011. In this work, only the residual biomass has been considered as a potential source of biomass gasification, in order to prevent soil utilization for dedicated fuel crops. In figure 3 are shown the regional distributions of residual biomass for each type of crops considered in the ENAMA study [37]: orchards, vineyards, cultivation of corn, sunflowers, and olives are considered. The residual biomass is converted to syngas through a gasification process based on the Viking two-stage gasifier developed by Denmark Technical University [38], operating with steam in the pyrolysis section, and with pure oxygen [33] in the gasification section. The operative scheme of the Viking gasifier is shown in figure 25.

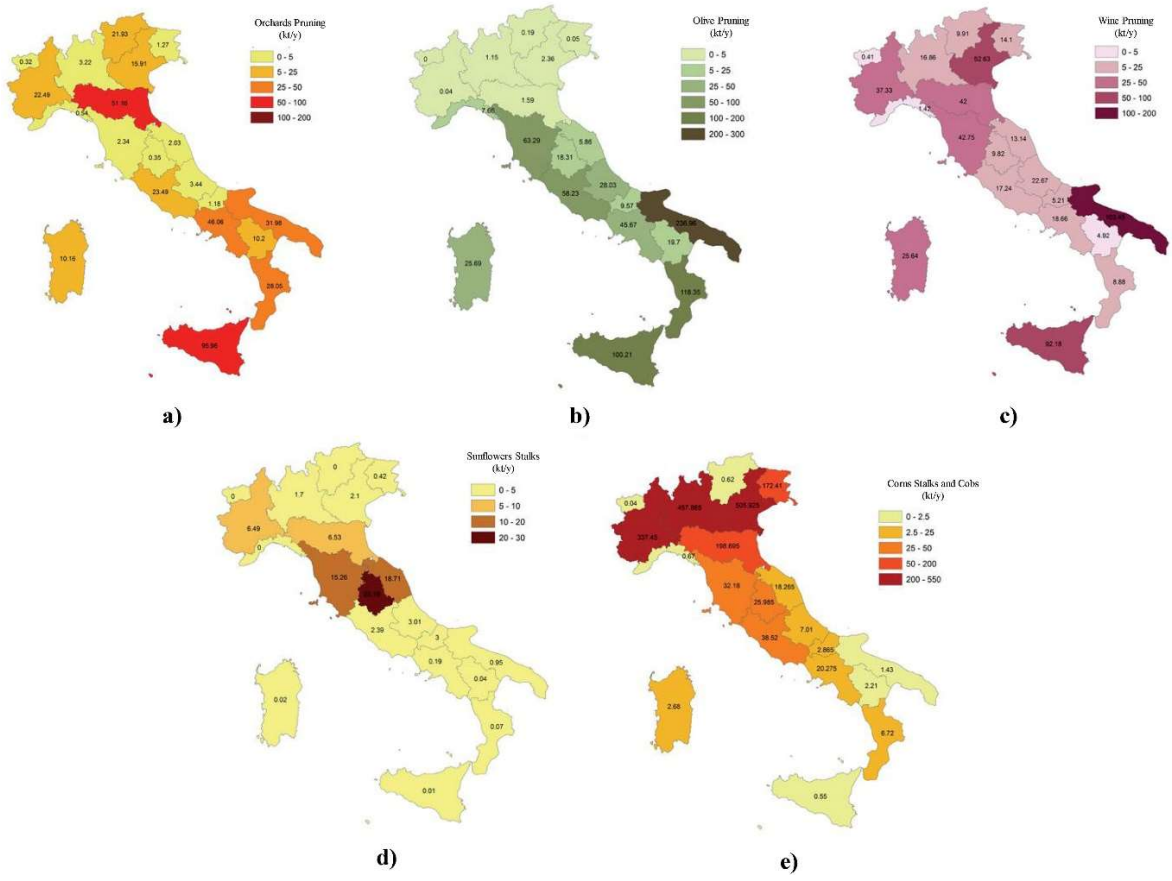

Figure 24. *Regional biomass availability – a) Orchards pruning – b) Olive pruning – c) Wine pruning – d) Sunflowers stalks – e) Corns stalks and cobs* [39]

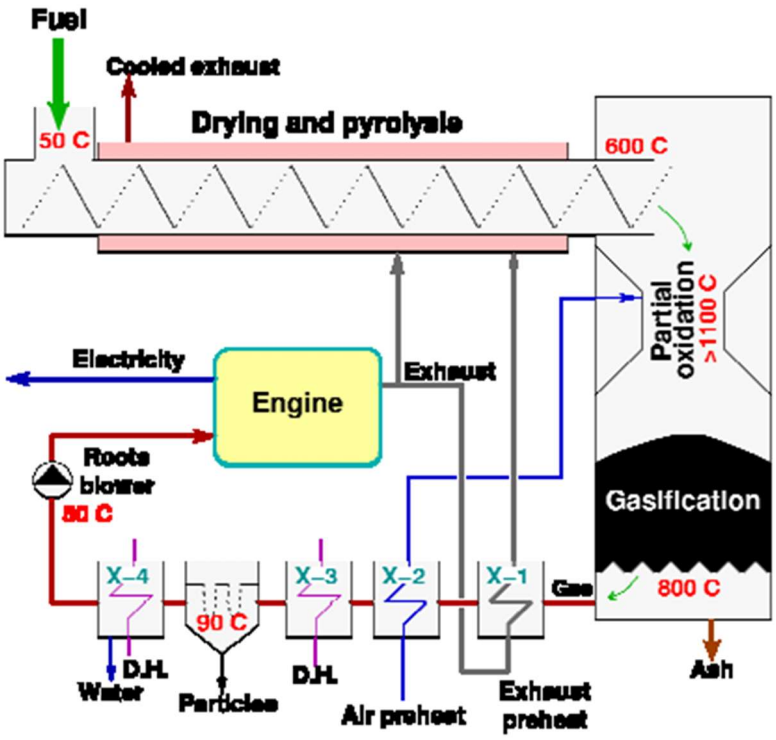

Figure 25. *Scheme of the Viking gasifier* [38]

The fact that it is a two-stage gasifier means that pyrolysis and char gasification occur in a separate reactor. During the pyrolysis, the biomass is brought into a pyrolysis reactor, where water evaporates, and the biomass is transformed into coke and tarry gas. Between the pyrolysis and gasification processes, the partial products are partially oxidized by air addition. This operation is able to reduce itself by a factor of 100 the tar production and makes available thermal energy for the endothermic char gasification. When the partially oxidized pyrolysis products pass through the char bed in the char gasification reactor, the tar contents are further reduced by a factor of 100. Finally, the gas is cooled down using a heat exchanger and the soot particles are gathered in a bag filter.

It has been assumed a gasification yield of 1.5 m^3/kg of dry syngas in normal conditions starting from dry biomass [40]. In table 8 the residual biomass availability and the corresponding dry syngas yield from the gasification process are reported.

Table 8. *Regional biomass availability and corresponding potential syngas yield* [37]

Region	Total available dry biomass [kt/y]	Dry syngas potential production [kt/y]
Piedmont	650	775
Aosta Valley	0.8	0.9
Lombardy	698	833
Trentino-S. T.	33	39
Veneto	669	799
Friuli V. Giulia	210	250
Liguria	10	12
Emilia Romagna	550	656
Tuscany	266	318
Umbria	145	173
Marche	189	226
Lazio	199	237
Abruzzo	100	120
Molise	56	67
Campania	175	209
Apulia	576	687
Basilicata	122	145
Calabria	196	234
Sicily	434	517
Sardinia	117	140
ITALY	*5,397*	*6,438*

5.2.2 Carbon Dioxide from biogas upgrade

In this work, three primary sources of biogas have been considered: the one available from anaerobic digestion of the organic fraction of the municipal solid waste (OFMW), the sludge from wastewater treatment plants (WWTP), and livestock manure. In order to consider the maximum quantity of CO_2 that could be recovered,

it has been made the hypothesis that all the manure produced by pigs and cattle farming at regional scale could be used for the purpose of this work. Data for livestock manure and wastewater treatment facilities have been taken from a study done by ENEA [41]. Conversely, the data for the OFMSW have been taken from the 2015 national report on municipal waster by ISPRA [42]. The total biogas that can be produced on a regional scale is reported in table 9.

Table 9. *Total biogas yield and corresponding recoverable CO_2*

Region	Biogas from pigs and cattle manure (Millions of Nm^3/y)	CO_2 from pigs and cattle manure (kt/y)	Biogas from WWTP (Millions of Nm^3/y)	CO_2 from WWTP (kt/y)	Biogas from OFMSW (Millions of Nm^3/y)	CO_2 from OFMSW (kt/y)
Piedmont	243	191	41	28	57	45
Aosta Valley	10	7.9	2	1.4	0.7	0.5
Lombardy	531	417	68	47	155	122
Trentino-S. T.	49	39	12	8.5	18	14
Veneto	172	135	48	33	98	77
Friuli V. Giulia	28	22	10	6.9	20	16
Liguria	4.7	3.1	9.5	6.5	10	7.9
Emilia Romagna	201	158	41	28	95	75
Tuscany	24	19	44	30	58	45
Umbria	18	14	4.1	2.8	14	11
Marche	19	15	10	6.9	30	24
Lazio	84	66	41	28	54	42
Abruzzo	22	17	11	7.4	18	14
Molise	13	10	5.4	3.7	1.5	1.1
Campania	120	95	43	30	95	75

Apulia	46	36	35	24	25	19
Basilicata	26	20	3.4	2.3	2.4	1.8
Calabria	43	34	10	7.1	6.8	5.3
Sicily	86	68	23	16	18	14
Sardinia	78	62	16	11	28	22
ITALY	*1,820*	*1,429*	*478*	*328*	*803*	*631*

Depending on the type of the source used for the biogas, two different compositions of it have been taken into account:

- in the case of biogas from wastewater sludge, the composition is considered to be 65% vol. of CH_4 and 35% vol. of CO_2 [43];
- in case of biogas derived from the OFMSW and the livestock manure, a composition of 60% vol. of CH_4 and 40% vol. of CO_2 has been considered (after the clean-up section).

In figure 26 the total regional yield of both CH_4 and CO_2 from biogas is represented. The CH_4 produced with this solution will be considered in the analysis in the following section.

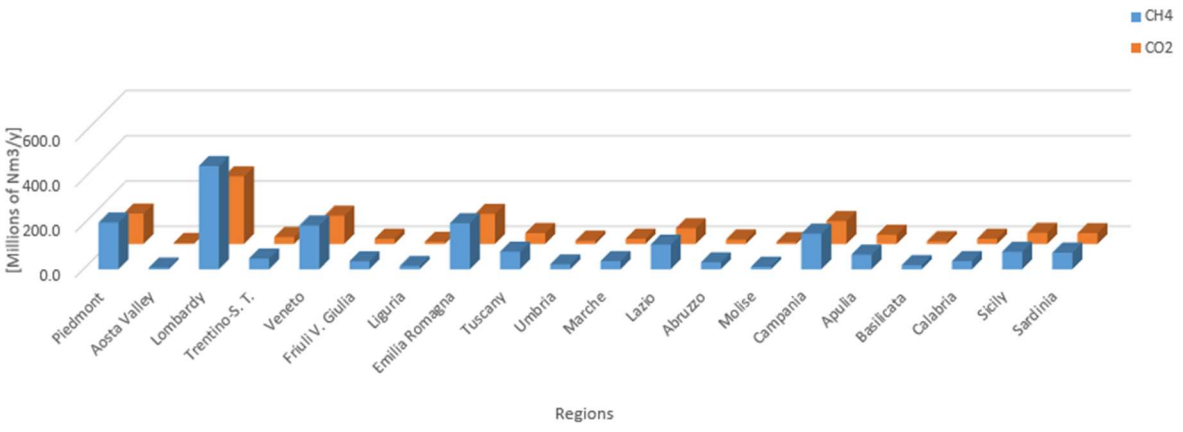

Figure 26. *Total regional yield of CH_4 and CO_2*

The process considered to separate the component of the biogas is an amine scrubbing technique: this kind of technologies consists in using a reagent that chemically binds to the CO_2 molecule, removing it from the gas. This is most generally performed

through a water solution of amines (molecules with carbon and nitrogen). The most common amines used historically for the purpose of sour gas removal (carbon dioxide and hydrogen sulphide) are methyldiethanolamine (MDEA), diethnolamine (DEA) and monoethanolamine (MEA) [44]. However the most common ammine used is a mixture of MDEA and piperazine (PZ) called aMDEA, that is the one considered in this work. The process using aMDEA essentially consists of two parts [44] (figure 27):

- an absorber, where the CO_2 and H_2S part of the biogas reacts with the amine and is transferred from the vapor to the liquid phase; being an exothermic reaction the absorption is favoured by high temperatures from a kinetic point of view, but by low temperature from a thermodynamic standpoint; the process is driven at 1-2 bar;
- a stripper, in which the CO_2 and H_2S is removed from the amine solution; the bottom part of it is equipped with a reboiler that brings the temperature to 120-150 °C by adding heat; this has a double intent: first it pushes the reaction of desorption towards the products, secondly it generates steam to lower the partial pressure of the CO_2 in the stripper, thus improving the kinetics of desorption; the process, in this case, is driven at 1.5-3 bar.

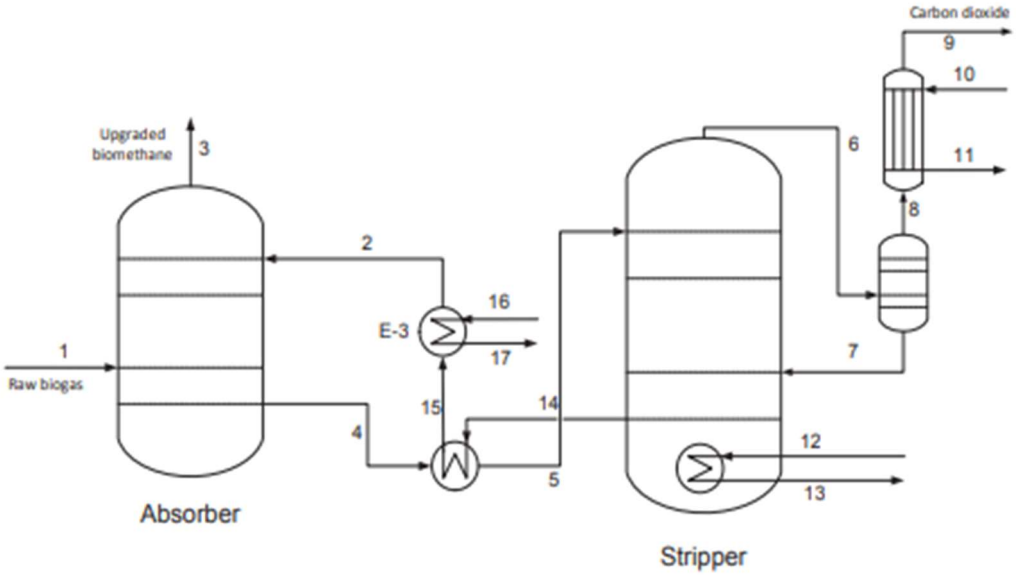

Figure 27. *Simplified process flow diagram of an amine scrubber for biogas upgrading* [45]

The process has an electrical consumption of 450 kJ and a heat demand of 2 MJ for the treatment of biogas corresponding to one cubic meter of methane [45]. A specific electric equivalent consumption (SEEC) of 2.5 MJ has been considered in the calculation of the energy consumption of the entire process.

5.2.3 Carbon dioxide from power plants' exhaust

The potential carbon dioxide that could be recovered from the exhaust of fossil-fueled power plants has been evaluated starting from the so-called emission factors that represent the amount of CO_2 released per unit of energy produced. The unit of measurement of it is [$ktCO_2/GWh$]. The emission factors are reported in table 10 [46]. The higher values could be seen in Liguria, Apulia and Tuscany, where mostly coal-fired and fuel oil power plants are present. Contrariwise in regions like Marche and Emilia Romagna, the emission factors are lower because of the greater presence of hydroelectric power plants. On the base of these emission factors, the CO_2 emissions in the year 2016 have been determined through the data about the regional thermoelectric production [47]. In table 10, besides the emission factors, the regional thermoelectric production and the corresponding CO_2-released are reported.

Table 10. *CO_2 emissions on regional base for the year 2016*

Region	Electrical Production [GWh/y]	Regional emission factors [kt/GWh]	CO_2 emissions [kt/y]
Piedmont	17,403	0.42	7,242
Aosta Valley	25	0.77	19
Lombardy	30,179	0.41	12,342
Trentino-S. T.	1571	0.40	626
Veneto	12,378	0.64	7,938
Friuli V. Giulia	8,565	0.67	5,773
Liguria	6,013	1.02	6,125
Emilia Romagna	19,191	0.36	6,992
Tuscany	9,325	0.80	7,488
Umbria	637	0.51	328
Marche	500	0.34	170
Lazio	18,157	0.52	9,375
Abruzzo	2,102	0.40	835
Molise	1,211	0.40	481
Campania	7,162	0.51	3,628
Apulia	27,016	0.93	25,177
Basilicata	576	0.47	268
Calabria	12,767	0.39	4,991
Sicily	15,478	0.62	9,573
Sardinia	9,175	0.63	5,737
ITALY	*199,430*	/	*115,109*

From a technical standpoint, the process considered to separate CO_2 from the total exhaust stream has been the Rectisol® Acid Gas Removal technology. As said before, the AGR unit is the name given to the unit where CO_2 and eventually H_2S are removed. A physical solvent is used to absorb the CO_2 and remove it from the syngas. The Rectisol® process foresees the use of chilled methanol for the absorption of both CO_2 and H_2S. The good thing about the Rectisol® process is that also other minor/trace impurities are removed from the syngas leaving at the outlet an ultra-clean syngas without sulfur and CO_2-free. Figure 30 shows how chilled methanol has a much higher absorption capacity for sulfur compounds (H_2S and COS) and CO_2 than for fuel compounds (CH_4, H_2 and CO) and N_2. So, methanol is a good solvent to capture H_2S and CO_2 from the syngas stream selectively. Furthermore, according to

figure 28, in order to increase the efficiency of the method, the temperature should be kept very low (-20÷-40 °C).

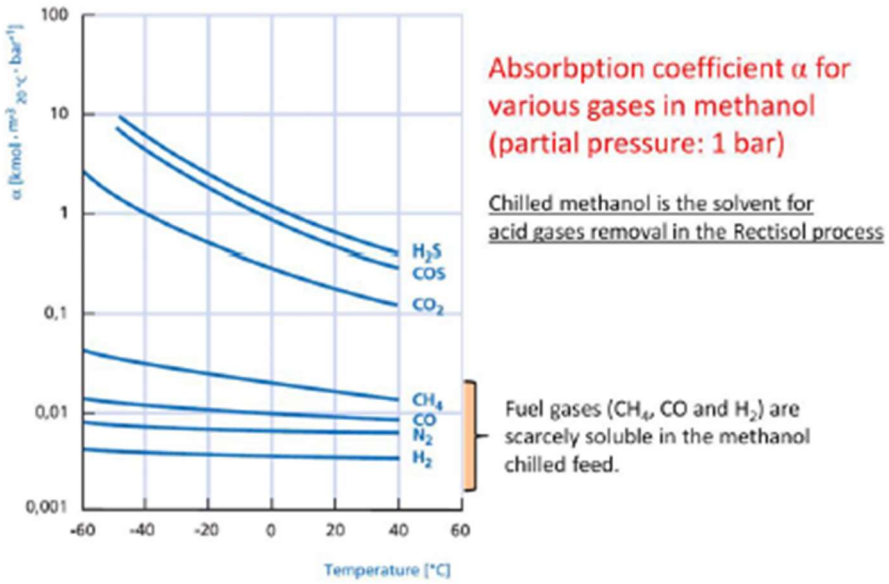

Figure 28. *Absorption coefficient for various gases in methanol wrt temperature* [48]

The functional scheme of a typical Rectisol® plant is shown in figure 29.

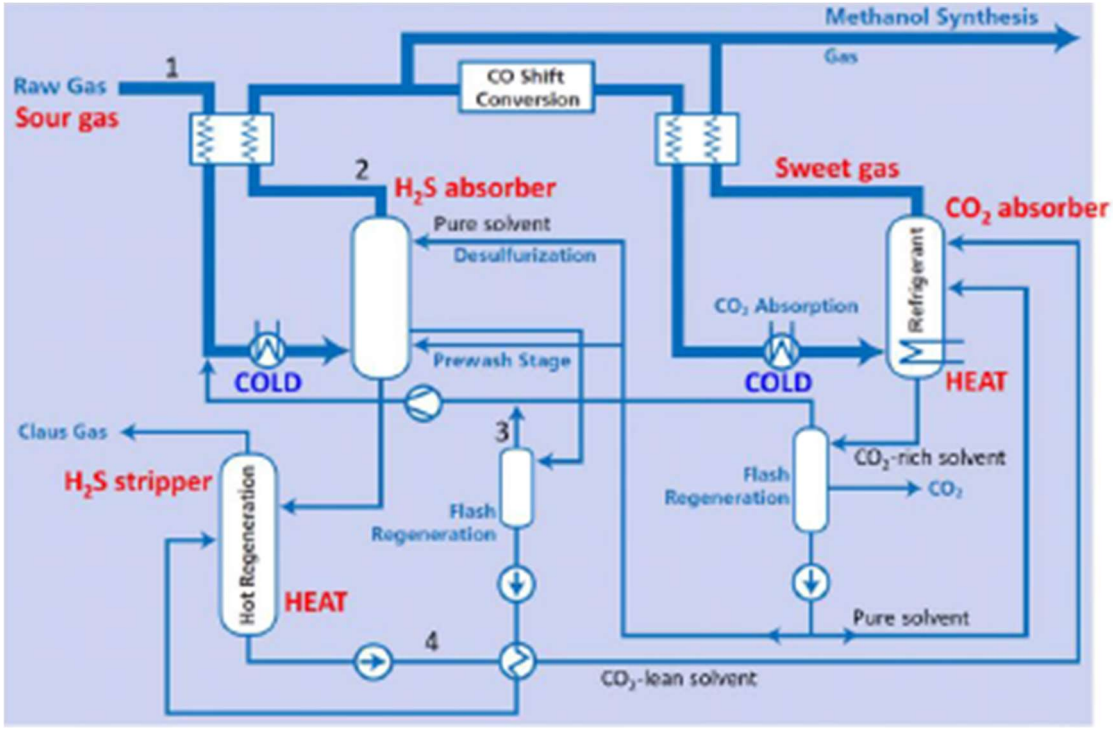

Figure 29. *Typical scheme of a Rectisol® plant* [44]

For the Rectisol® process, a percentage of CO_2 recovered of 95% and a SEEC of 925 kJ/kg that incorporates both electrical and thermal energy demand have been considered [49].

5.2.4 Water resources availability

The water is essential in the processes involved in this work, and due to its high availability, it is never a limiting factor in the calculation presented in the following section. In table 11 the regional availability of the water for the year 2015 is reported.

Table 11. *Regional water availability* [50]

Region	Water dispensed by public network [kt/y]	Water admitted in the public network [kt/y]
Piedmont	378	584
Aosta Valley	21	26
Lombardy	993	1,392
Trentino-S. T.	112	160
Veneto	388	648
Friuli V. Giulia	102	196
Liguria	160	239
Emilia Romagna	326	471
Tuscany	241	427
Umbria	54	102
Marche	110	167
Lazio	458	973
Abruzzo	120	231
Molise	28	53
Campania	437	820
Apulia	231	427
Basilicata	43	98
Calabria	206	350

Sicily	342	683
Sardinia	122	275
ITALY	*4,875*	*8,320*

In order to not perturb the balance of water dispensed by the public network, in this work the effective availability of water is given by the difference between the water admitted in the public network and the water dispensed by the public network.

5.2.5 Renewable electricity availability

The data about the availability of the renewable electricity on the regional scale have been provided by the report made by the Italian Institution for the Management of the Energetic Services (GSE) in which the renewable energy produced by each type of renewable source during the year 2016 is reported. In table 12 these data are summarized.

The use of the electricity coming from the renewable energy sources has been considered mandatory in this work, both because of the difficulty in the displacement of this kind of energy and because of the will of maintaining this process as "green" as possible thus not considering ways for the production of electric energy that involve GHG emission.

Table 12. *Renewable electricity production for the year 2016* [51]

Region	Hydroelectric [GWh/y]	Wind [GWh/y]	Photovoltaic [GWh/y]	Geothermal [GWh/y]	Total [GWh/y]
Piedmont	6,524.1	30.2	1,688.1	/	8,242.4
Aosta Valley	2,993.3	4.0	25.1	/	3,022.4
Lombardy	9,786.3	-	2,167.7	/	11,954.0
Trentino-S. T.	8,781.5	0.1	432.9	/	9,214.5
Veneto	3,839.5	16.1	1,886.1	/	5,741.7

Friuli V. Giulia	1,588.5	-	520.2	/	2,108.7
Liguria	219.6	130.8	103.2	/	453.6
Emilia Romagna	904.9	34.6	2,093.7	/	3,033.2
Tuscany	839.7	237.6	869.8	6,288.6	8,235.7
Umbria	1,434.2	3.2	520.3	/	1,957.7
Marche	603.7	17.1	1,222.4	/	1,843.2
Lazio	977.5	98.0	1,503.4	/	2,578.9
Abruzzo	1,585.6	374.9	830.9	/	2,791.4
Molise	203.1	709.6	208.4	/	1,121.1
Campania	500.6	2,562.3	834.5	/	3,897.4
Apulia	3.8	4,794.0	3,464.6	/	8,262.4
Basilicata	268.7	1,571.8	447.0	/	2,287.5
Calabria	1,075.7	2,174.4	616.7	/	3,866.8
Sicily	142.4	3,058.0	1,744.4	/	4,944.8
Sardinia	159.1	1,872.0	925.0	/	2,956.1
ITALY	*42,431.8*	*17,688.7*	*22,104.4*	*6,288.6*	*88,513.5*

5.3 Summary of the pathways for fuel production

In table 13 the pathways for fuel production are summarized.

Table 13. *Pathways for fuel production*

Pathway	Source	Process	Upgrade Technology	Synthesis	Final Product
1	Residual biomass sources	Biomass Gasification	SOEC co-electrolysis	Methanation	Synthetic Natural Gas
2	Biogas off-gas after upgrading to biomethane	CO_2 separation via amine scrubbing			
3	Exhaust gas of fossil power plants	CO_2 separation via Acid Gas Removal Process (Rectisol®)			
4	Water from public network	/	SOEC electrolysis	/	Hydrogen

6. Results

In this work four main scenarios have been analyzed, with minor sub-scenarios for some of this:

- SNG production from gasified residual biomass;
- SNG production from CO_2 recovered from biogas upgrade;
- SNG production from CO_2 recovered from thermoelectric power plant exhaust;
- Hydrogen production from water from the public network.

For each case a conversion efficiency has been computed, according to equations (37), (38) and (39):

$$\eta_{SNG\ from\ CO_2} = \frac{M_{SNG} \cdot LHV_{SNG}}{E_{SOEC} + E_{Aux} + E_{sep,CO_2}} \quad \textbf{(37)}$$

$$\eta_{SNG\ from\ biomass} = \frac{M_{SNG} \cdot LHV_{SNG}}{E_{SOEC} + E_{Aux} + M_{biomass} \cdot LHV_{biomass}} \quad \textbf{(38)}$$

$$\eta_{H_2} = \frac{M_{H_2} \cdot LHV_{H_2}}{E_{SOEC} + E_{Aux} + Q} \quad \textbf{(39)}$$

In equation (38) the value considered for $LHV_{biomass}$ has been 17.9 MJ/kg [37]; this is the mean value of all the minimum and maximum values of all the type of biomass considered in this work.

In the previous equation in the denominator doesn't appear the heat that should be used for the steam production as well as for the pre-heat of the flows entering the SOEC. This because the heat of reaction generated from the synthesis process (equations (23) and (24)) is sufficient to cover the heat for steam production (31.8 kJ/mol at 33 bar). Moreover, the heat needed for the pre-heat of the flows entering the SOEC is considered to be recovered by the same SOEC outlet flow [52]. For these reasons the thermal energy related to the production of SNG has not been considered in the external energy demand. Furthermore, since this analysis does not deal with the design of a real plant, a pinch analysis has not been performed.

However, in case of steam electrolysis, the heat used to bring the temperature of the pressurized water to the designed SOEC inlet temperature cannot be completely

recovered from the exiting streams, so it has been taken into account in the total energy expenditure balance. For the sake of simplicity, the assumption of a 100% efficiency of conversion of electricity into heat has been made.

For each case, regarding the calculation of the overall national data, these last ones have been considered as the algebraic sum of the data of all the regions.

Finally, the hypothesis of 90% of total hours of the year of system working has been made (i.e., 7884 h).

6.1 SNG from CO_2

6.1.1 SNG from CO_2 recovery from biogas upgrade off-gas

In this case, two specific sub-cases have been analyzed:

- The first in which is considered only the SNG produced by the CO_2 recovered from the syngas (case 1a);
- The second in which, aside from the SNG produced by the CO_2 from the syngas, is also considered the CH_4 produced by the biogas, with the hypothesis that it can be totally used for the purposes of this work (case 1b).

In table 14 the results related to the first sub-case are shown.

Table 14. *Results in case of exploitation only of CO_2*

Region	Input			Output		
	CO_2 from biogas upgrade [kt/y]	**Total electrical demand [GWh/y]**	**Share of RES-electricity consumed [%]**	**SNG production [kt/y]**	**Share of the demand covered by SNG [%]**	**Conversion Efficiency (Eq. (37))**
Piedmont	264	1,742	21.1	100	10.6	76.02
Aosta Valley	9.8	64	2.1	4	10.0	
Lombardy	586	3,866	32.3	221	10.6	

Trentino-S. T.	61	404	4.4	23	8.9	
Veneto	246	1,623	28.3	93	8.1	
Friuli V. Giulia	45	296	14.0	17	3.6	
Liguria	18	117	25.7	7	7.1	
Emilia Romagna	261	1,720	56.7	99	4.5	
Tuscany	95	627	7.6	36	5.1	
Umbria	28	185	9.4	11	5.3	
Marche	46	302	16.4	17	6.1	
Lazio	136	902	35.0	52	10.5	
Abruzzo	39	255	9.1	15	5.6	
Molise	15	99	8.8	6	35.9	
Campania	199	1,313	33.7	75	21.1	
Apulia	80	527	6.4	30	4.4	
Basilicata	24	160	7.0	9	6.4	
Calabria	46	305	7.9	17	54.0	
Sicily	97	643	13.0	37	5.6	
ITALY	*2,294*	*15,150*	*17.1*	*867*	*7.8*	

In table 15 the results related to the exploitation of the CH_4 from biogas are shown. The other input data, being the same, have been omitted.

Table 15. *Results in the case of exploitation also of the SNG from biogas upgrade*

Region	Input	Output	
	SNG from biogas upgrade [kt/y]	SNG total production [kt/y]	Share of the demand covered by total SNG [%]
Piedmont	148	247	26.9
Aosta Valley	5	9	25.6
Lombardy	326	547	27.1
Trentino-S. T.	34	58	22.7
Veneto	138	231	20.7
Friuli V. Giulia	25	42	9.2
Liguria	10	17	18.8
Emilia Romagna	146	244	11.5
Tuscany	56	91	13.4
Umbria	16	26	13.6
Marche	26	43	15.5
Lazio	78	130	27.1
Abruzzo	22	37	14.4
Molise	9	14	93.2
Campania	112	187	54.1
Apulia	46	77	11.4
Basilicata	14	23	16.3
Calabria	26	44	100.0
Sicily	55	92	14.3
ITALY	*1,292*	*2,159*	*20.1*

From the results it is evident that this solution, in both sub-cases, does not ensure a sufficient coverage of the demand, so the limiting factor is the carbon dioxide itself: at the national level in the first case the covered demand is around 7.8% while in the second is 20.1%. However, in no region there was need of additional electric energy to process all the CO_2 recovered. It can be noticed that in the second case in one region,

i.e., Calabria, the demand is fully satisfied with a surplus of 2.96 kt of SNG that can turn out either in using this amount of SNG for other purposes or in saving electricity from RES thus converting less CO_2.

6.1.2 SNG from CO_2 recovery from thermoelectric power plant exhaust

In this specific case the amount of CO_2 recoverable is dramatically higher than the previous case, so three sub-cases have been taken into account:

- first case in which over-production and integration with electric energy from the grid have been considered (case 2a);
- second case in which over-production is not considered while integration with electric energy from the grid is still taken into account (case 2b);
- third case in which only the exploitation of electricity from V-RES has been considered (case 2c).

In table 16 (a and b) the results of the first case are showed.

Table 16a. *Results with over-production and integration of electric energy (Input)*

Region	Input			
	CO_2 from power plant exhaust [kt/y]	Total electrical demand [GWh/y]	Share of RES-electricity consumed [%]	Integration of electric energy from the grid [GWh/y]
Piedmont	6,880	43,553	100.0	35,311
Aosta Valley	18	115	3.8	/
Lombardy	11,725	74,229	100.0	62,275
Trentino-S. T.	595	3,764	40.8	/
Veneto	7,541	47,742	100.0	42,000
Friuli V. Giulia	5,484	34,717	100.0	32,608
Liguria	5,819	36,836	100.0	36,382
Emilia Romagna	6,643	42,053	100.0	39,020
Tuscany	7,114	45,035	100.0	36,799
Umbria	311	1,972	100.0	14
Marche	162	1,024	55.6	/
Lazio	8,906	56,382	100.0	53,803
Abruzzo	793	5,020	100.0	2,229

Molise	457	2,890	100.0	1,769
Campania	3,447	21,821	100.0	17,923
Apulia	23,918	151,419	100.0	143,156
Basilicata	255	1,613	70.5	/
Calabria	4,741	30,015	100.0	26,148
Sicily	9,094	57,570	100.0	52,625
ITALY	*103,903*	*657,769*	*100.0*	*582,062*

Table 16b. *Results with over-production and integration of electric energy (Output)*

Region	**Output**			
	SNG production [kt/y]	**Share of the demand covered by SNG [%]**	**SNG over-production [kt/y]**	**Conversion efficiency (Eq. (37))**
Piedmont	2,602	100.0	1,658	79.36
Aosta Valley	7	18.7	/	
Lombardy	4,435	100.0	2,359	
Trentino-S. T.	225	86.2	/	
Veneto	2,852	100.0	1,703	
Friuli V. Giulia	2,074	100.0	1,604	
Liguria	2,201	100.0	2,108	
Emilia Romagna	2,513	100.0	321	
Tuscany	2,691	100.0	1,990	
Umbria	118	59.3	/	
Marche	61	21.5	/	
Lazio	3,369	100.0	2,878	
Abruzzo	300	100.0	38	
Molise	173	100.0	157	
Campania	1,304	100.0	948	
Apulia	9,047	100.0	8,358	

Basilicata	96	67.5	/	
Calabria	1,793	100.0	1,761	
Sicily	3,440	100.0	2,777	
ITALY	*39,301*	*100.0*	*28,659*	

In this sub-case, it can be seen that, with the integration of electricity from the grid, the demand is fully covered in fourteen regions out of nineteen, and even at the national level the demand is fully satisfied. However, the dimension of the over-production of SNG is huge, so this solution is suitable only if this surplus could be exploited in other ways; otherwise the share of CO_2 converted can be decreased in order to reduce to the minimum the integration with the electricity from the grid, that conflicts with the assumption made at the beginning of this work.

Table 17 (a and b) shows the results of the second sub-case in which the over-production is not considered.

Table 17a. *Results without over-production but integration of electric energy (Input)*

Region	**Input**			
	CO_2 needed from power plant exhaust [kt/y]	**Total electrical demand [GWh/y]**	**Share of RES-electricity consumed [%]**	**Integration of electric energy from the grid [GWh/y]**
Piedmont	2,597	16,443	100.0	8,201
Aosta Valley	18	115	3.8	0
Lombardy	5,708	36,136	100.0	24,182
Trentino-S. T.	595	3,764	40.8	0
Veneto	3,160	20,006	100.0	14,265
Friuli V. Giulia	1,293	8,187	100.0	6,078
Liguria	257	1,625	100.0	1,171
Emilia Romagna	6,026	38,146	100.0	35,113
Tuscany	1,928	12,207	100.0	3,971

Umbria	311	1,972	100.0	14
Marche	162	1,024	55.6	0
Lazio	1,349	8,537	100.0	5,958
Abruzzo	721	4,565	100.0	1,773
Molise	43	273	24.4	0
Campania	979	6,196	100.0	2,299
Apulia	1,895	11,996	100.0	3,734
Basilicata	255	1,613	70.5	0
Calabria	89	563	14.6	0
Sicily	1,821	11,527	100.0	6,582
ITALY	*29,207*	*184,897*	*100.0*	*96,383*

Table 17b. *Results without over-production but integration of electric energy (Output)*

Region	**Output**		
	SNG production [kt/y]	**Share of the demand covered by SNG [%]**	**Conversion efficiency (Eq. (37))**
Piedmont	945	100.0	76.31
Aosta Valley	7	18.7	
Lombardy	2,076	100.0	
Trentino-S. T.	216	86.2	
Veneto	1,149	100.0	
Friuli V. Giulia	470	100.0	
Liguria	93	100.0	
Emilia Romagna	2,191	100.0	
Tuscany	701	100.0	
Umbria	113	59.3	
Marche	59	21.5	
Lazio	490	100.0	
Abruzzo	262	100.0	

Molise	16	100.0	
Campania	356	100.0	
Apulia	689	100.0	
Basilicata	93	67.5	
Calabria	32	100.0	
Sicily	662	100.0	
ITALY	*10,622*	*96.1*	

In this case, the quote of electrical energy supplied by the grid is considerably reduced and the conversion efficiency is slightly reduced.

Table 18 (a and b) shows the last results, where the integration of electricity from the grid is not considered.

Table 18a. *Results of the case without integration of electricity (Input)*

Region	Input		
	CO_2 from power plant exhaust converted [kt/y]	**Total electrical demand [GWh/y]**	**Share of RES-electricity consumed [%]**
Piedmont	1,302	8,242	100.0
Aosta Valley	18	115	3.8
Lombardy	1,889	11,954	100.0
Trentino-S. T.	595	3,762	40.8
Veneto	907	5,742	100.0
Friuli V. Giulia	333	2,109	100.0
Liguria	72	454	100.0
Emilia Romagna	479	3,033	100.0
Tuscany	1,301	8,236	100.0
Umbria	309	1,958	100.0
Marche	162	1,024	55.6
Lazio	408	2,579	100.0
Abruzzo	441	2,791	100.0

Molise	177	1,121	100.0
Campania	616	3,897	100.0
Apulia	1,306	8,262	100.0
Basilicata	255	1,613	70.5
Calabria	611	3,867	100.0
Sicily	781	4,945	100.0
ITALY	*11,963*	*75,704*	*85.5*

Table 18b. *Results of the case without integration of electricity (Output)*

Region	Output			
	SNG production [kt/y]	Share of the demand covered by SNG [%]	SNG over-production [kt/y]	Conversion efficiency (Eq. (37))
Piedmont	493	52.2	/	79.39
Aosta Valley	7	18.7	/	
Lombardy	714	34.4	/	
Trentino-S. T.	225	86.2	/	
Veneto	343	29.9	/	
Friuli V. Giulia	126	26.8	/	
Liguria	27	29.0	/	
Emilia Romagna	181	8.3	/	
Tuscany	492	70.2	/	
Umbria	117	58.9	/	
Marche	61	21.5	/	
Lazio	154	31.4	/	
Abruzzo	167	63.6	/	
Molise	67	100.0	67	
Campania	233	65.4	/	
Apulia	494	71.7	/	

Basilicata	96	67.5	/	
Calabria	231	100.0	231	
Sicily	296	44.6	/	
ITALY	*4,525*	*40.9*	*298*	

In this last case only in two regions, i.e., Molise and Calabria, the demand is fully covered even with a surplus of SNG produced. This last solution seems to be the best one according to the assumption of this work, since only electricity from V-RES is used, and the percentages of demand satisfied are relatively high.

6.1.3 SNG from syngas from residual biomass gasification

In this section, the results for SNG production from syngas from residual biomass gasification are presented and commented (case 3). The results are summarized in table 19.

Table 19. *Results of SNG from biomass gasification*

Region	Input			Output		
	Syngas from biomass gasification [kt/y]	Total electrical demand [GWh/y]	Share of RES-electricity consumed [%]	SNG production [kt/y]	Share of the demand covered by SNG [%]	Conversion Efficiency (Eq. (38))
Piedmont	775	3,195	38.8	352	37.3	72.83
Aosta Valley	0.9	4	0.1	0.4	1.1	
Lombardy	833	3,432	28.7	378	18.2	
Trentino-S. T.	39	161	1.8	18	6.8	
Veneto	799	3,292	57.3	363	31.6	
Friuli V. Giulia	250	1,032	49.0	114	24.2	
Liguria	12	51	11.3	5.6	6.1	
Emilia Romagna	656	2,704	89.2	298	13.6	
Tuscany	318	1,310	15.9	144	20.6	
Umbria	173	713	36.4	79	39.6	
Marche	226	930	50.5	102	36.0	
Lazio	237	978	37.9	108	22.0	
Abruzzo	120	493	17.7	54	20.7	
Molise	67	276	24.6	30	100.0	
Campania	209	861	22.1	95	26.7	

Apulia	687	2,831	34.3	312	45.3	
Basilicata	145	599	26.2	66	46.2	
Calabria	234	965	24.9	106	100.0	
Sicily	517	2,133	43.1	235	35.5	
ITALY	*6,298*	*25,961*	*29.3*	*2,859*	*25.9*	

In this case, in no region there is total exploitation of the V-RES, so the integration of electricity with the one from the grid is not requested. The percentages of coverage of the demand are relatively small even if in two regions, i.e., Calabria and Molise, like in the third case of the previous scenario, the demand is fully covered with a surplus of SNG respectively of 74 and 15 kt.

In the computation of the energy expenditure, the gathering of the residual biomass has not been taken into account; this would further increase the total energy consumption.

6.2 Hydrogen from water from the public network

Analogously as the case of CO_2 recovery from thermoelectric power plants exhaust two sub-cases have been studied:

- first case in which the demand is assumed to be fully satisfied with integration of electricity from the grid (case 4a);
- second case in which the electricity from V-RES has been imposed as a limiting factor (case 4b).

In table 20 the results of the first case have been summarized.

Table 20. *Results of H_2 production with the integration of electricity*

Region	Input				Output	
	H_2O needed from public network [kt/y]	Total electrical demand [GWh/y]	Share of RES-electricity consumed [%]	Integration of electric energy from the grid [GWh/y]	H_2 production [kt/y]	Conversion efficiency (Eq. (39))
Piedmont	4,612	17,430	100.0	9,188	377	71.99
Aosta Valley	180	681	22.5	0	15	
Lombardy	10,136	38,305	100.0	26,351	828	
Trentino-S. T.	1,273	4,812	52.2	0	104	
Veneto	5,612	21,207	100.0	15,465	458	
Friuli V. Giulia	2,296	8,678	100.0	6,569	188	
Liguria	456	1,722	100.0	1,269	37	
Emilia Romagna	10,699	40,435	100.0	37,402	874	
Tuscany	3,424	12,940	100.0	4,704	280	
Umbria	970	3,664	100.0	1,707	79	

Marche	1,391	5,258	100.0	3,414	114	
Lazio	2,394	9,049	100.0	6,470	196	
Abruzzo	1,280	4,839	100.0	2,047	105	
Molise	77	290	25.8	0	6	
Campania	1,738	6,568	100.0	2,671	142	
Apulia	3,365	12,717	100.0	4,454	275	
Basilicata	698	2,636	100.0	349	57	
Calabria	158	597	15.4	0	13	
Sicily	3,233	12,219	100.0	7,274	264	
ITALY	*53,992*	*204,047*	*100.0%*	*115,534*	*4,410*	

In this case, it can be observed that in 4 regions out of 19, i.e., Aosta Valley, Trentino S.T., Calabria and Molise, the demand is fully satisfied with a partial utilization of the electricity from V-RES. However, this solution does not result to be suitable because the share of electricity that should be integrated from the grid is a huge part of the total, and as previously mentioned, this conflicts with the initial purposes of this work.

In table 21 the results of the case with electricity from V-RES as limiting factor.

Table 21. *Results of H_2 production without integration of electricity*

Region	**Input**			**Output**		
	H_2O needed from public network [kt/y]	**Total electrical demand [GWh/y]**	**Share of RES-electricity consumed [%]**	**H_2 production [kt/y]**	**Share of the demand covered by H_2 [%]**	**Conversion efficiency (Eq. (39))**
Piedmont	2,181	8,242	100.0	178	47.3	71.99
Aosta Valley	180	681	22.5	15	100.0	
Lombardy	3,163	11,954	100.0	258	31.2	

Trentino-S. T.	1,273	4,812	52.2	104	100.0	
Veneto	1,519	5,742	100.0	124	27.1	
Friuli V. Giulia	558	2,109	100.0	46	24.3	
Liguria	120	454	100.0	10	26.3	
Emilia Romagna	803	3,033	100.0	66	7.5	
Tuscany	2,179	8,236	100.0	178	63.6	
Umbria	518	1,958	100.0	42	53.4	
Marche	488	1,843	100.0	40	35.1	
Lazio	682	2,579	100.0	56	28.5	
Abruzzo	739	2,791	100.0	60	57.7	
Molise	77	290	25.8	6	100.0	
Campania	1,031	3,897	100.0	84	59.3	
Apulia	2,186	8,262	100.0	179	65.0	
Basilicata	605	2,287	100.0	49	86.8	
Calabria	158	597	15.4	13	100.0	
Sicily	1,306	4,935	100.0	107	40.4	
ITALY	*19,767*	*74,702*	*84.4*	*1,615*	*36.6*	

In this case, the values of covered demand are not so high but considering that this is a completely zero-carbon fuel these data could be considered a good result in this framework.

6.3 Comparison between the different scenarios

It is useful to make a comparison between the various scenarios on the overall national level, based mainly on the percentage of demand covered, the exploitation of electricity from V-RES and the conversion efficiency. In table 25 (a and b) the comparisons are summarized.

Table 22a. *Comparison between the different scenarios (Input)*

Case	INPUT			
	Syngas upgraded, or CO_2/H_2O converted [kt/y]	**Total energy demand [GWh/y]**	**Share of RES-electricity consumed [%]**	**Integration with electricity from the grid [GWh/y]**
SNG from biogas recovered CO_2 (1a)	2,294	15,150	17.1	/
SNG from biogas recovered CO_2 + SNG from biogas (1b)	2,294	15,150	17.1	/
SNG from exhaust recovered CO_2 with integration of electricity and over-production (2a)	103,903	657,769	100.0	582,602

SNG from exhaust recovered CO_2 with integration of electricity and no over-production (2b)	29,207	184,897	100.0	96,383
SNG from exhaust recovered CO_2 without integration of electricity (2c)	11,963	75,704	85.5	/
SNG from gasified biomass upgrade (3)	6,298	25,961	29.3	/
Hydrogen with integration of electricity (4a)	53,992	204,047	100.0	115,534
Hydrogen without integration of electricity (4b)	19,767	74,702	84.4	/

Table 22b. *Comparison between the different scenarios (Output)*

Case	OUTPUT			
	Synfuel production [kt/y]	**Demand covered with synfuel [%]**	**Synfuel over production [kt/y]**	**Conversion efficiency**
SNG from biogas recovered CO_2 (1a)	867	7.8	/	76.02
SNG from biogas recovered CO_2 + SNG from biogas (1b)	2,159	20.1	/	76.02
SNG from exhaust recovered CO_2 with integration of electricity and over-production (2a)	39,301	100.0	28,659	79.36
SNG from exhaust recovered CO_2 with integration of electricity and no over-production (2b)	10,622	96.1	/	76.31

SNG from exhaust recovered CO_2 without integration of electricity (2c)	4,525	40.9	/	79.39
SNG from gasified biomass upgrade (3)	2,859	25.9	/	72.83
Hydrogen with integration of electricity (4a)	4,410	100.0	/	71.99
Hydrogen without integration of electricity (4b)	1,615	84.4	/	71.99

In figure 24 and 25 a visual comparison among the different percentages of covered demand is shown. It is useful to divide the cases into two macro-groups, the cases which contemplate the integration of electricity from the grid and the cases which do not contemplate the integration of electricity from the grid. This split is done because the cases of the second macro-group are more meaningful for the purposes of this work.

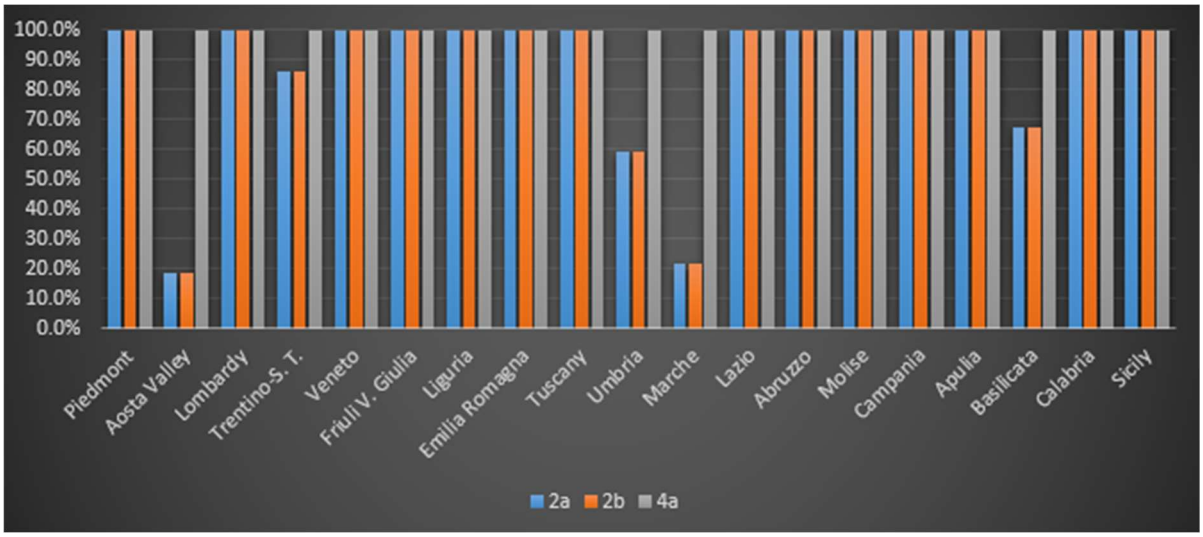

Figure 30. *Comparison among all the regions (cases with the integration of electricity)*

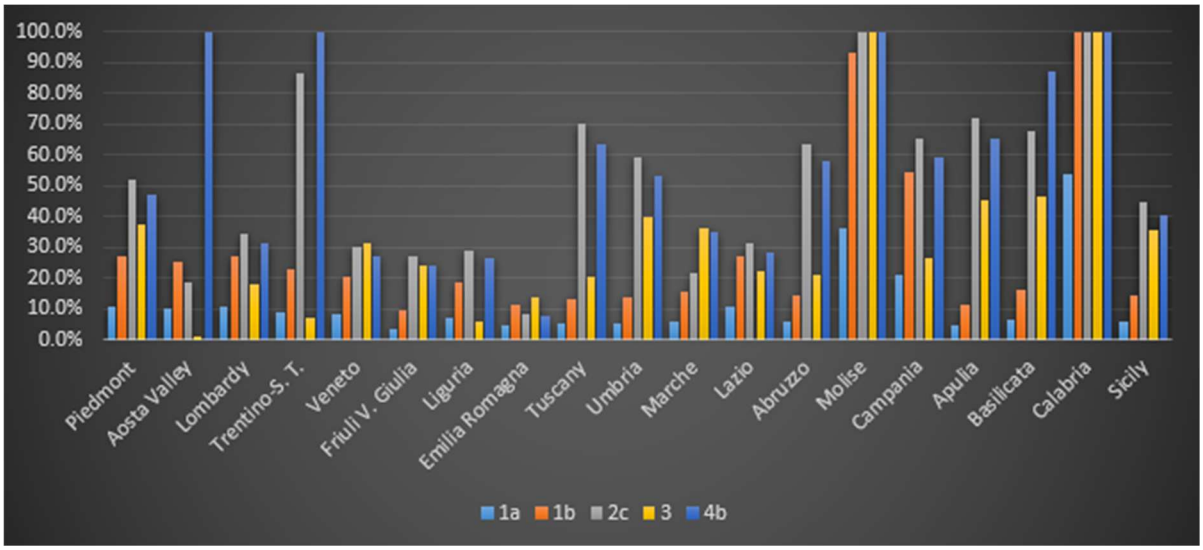

Figure 31. *Comparison among all the regions (cases without integration of electricity)*

It can be seen that in the cases with the integration of electricity, almost always the demand is fully covered; however, these cases have been studied for completeness, but actually they violate the main assumption made in the introduction of this work, i.e., the exclusive usage of electricity from V-RES.

Through the tabular and visual comparisons, the best case turns out to be the case 4b, but as said before, the difficulties relative to the effective exploitation of the hydrogen as a fuel must be outdone.

Conclusions

In this work, the production of synfuels for fossil fuel substitution in the industrial sector, starting from the different feedstock, has been investigated considering the Italian industrial demand aggregated at the regional scale. From the results it is clear that the limiting factor in most of the cases is the electricity from V-RES, especially in the case of the SNG from exhaust recovered and the H_2: in fact, in these cases, with the adequate amount of electric energy, the demand would be fully fulfilled. The most promising case results to be the 4b (hydrogen without integration of electricity), that at a national level would cover almost the 85% of the demand, but in this case, as always remarked in this work, there are difficulties arisen from the effective dispatching and exploitation of the hydrogen as a fuel. Regarding SNG the greatest plenitude of feedstock is given by the exhaust recovered CO_2, which, in case of full availability of electricity would satisfy all the demand even with a surplus of SNG produced; in case of exploitation of only V-RES, the demand coverage would be around 40%; although this solution would be the best in the case of accomplishment of a carbon-neutral way to produce natural gas, it is necessary to specify that the infrastructure necessary to collect the produced CO_2 is still missing. Moreover, from the conversion efficiency standpoint the SNG production results more performing than the H_2 production. In summary it can be said that in the next future, with an effort on the accomplishment of proper infrastructures, these solutions could become of great interest.

Acknowledgements

Con questo lavoro si conclude un percorso lungo e non privo di insidie iniziato più di 5 anni fa, un percorso nel quale non ho solamente acquisito mere conoscenze, ma sono cresciuto e maturato come persona. Da ogni persona che ha attraversato il mio percorso ho cercato di mutuare le cose migliori, e ciascuna di esse mi ha arricchito e cambiato a modo suo.

Ringrazio il Prof. Santarelli per avermi concesso la possibilità di dedicarmi a questo lavoro e per avermi invogliato in principio con l'insegnamento della sua materia ad appassionarmi a questo ramo e ad aprirmi nuovi orizzonti.

Ringrazio in particolare i miei genitori, che oltre al materiale supporto economico hanno sempre tenuto ad inculcarmi i valori di onestà e sacrificio; se sono diventato quello che sono oggi è soprattutto grazie a loro.

Ringrazio tutti i colleghi, in particolare il mio perpetuo compagno di studi Antonio e i cari baresi, per aver reso questi anni di studio meno pesanti grazie alla costante componente goliardica.

Ringrazio tutti gli amici che sono stati presenti in questi anni, con particolare menzione al "gruppo del parco", la mia vera cura nei momenti meno facili.

Ringrazio in generale chiunque mi abbia sempre supportato incondizionatamente e chiunque abbia creduto ciecamente in me e a tutti questi dedico questo lavoro e la mia carriera universitaria.

References

[1] I. Dincer, G. Naterer, "Novel Hydrogen Production Technologies and Applications";

[2] E. Giglio, M. Santarelli, A. Lanzini, "Modelling of high-temperature electrolysis and methanation processes for synthetic natural gas production";

[3] "*L'idrogeno Da Rinnovabili Sarà Mai Competitivo Con Il Gas Naturale? Cosa Dicono Le Ultime Ricerche*", available at: http://www.qualenergia.it;

[4] A. Godula-Jopek, "Hydrogen production by electrolysis";

[5] A. Varone, M. Ferrari, "Power to liquid and power to gas: an option for the German *Energiewende*";

[6] M. Götz et al., "Renewable Power-to-Gas: a technological and economic review";

[7] R. Tilagone, "*Gaz naturel – Énergie fossile, Techniques de l'ingénieur*";

[8] L. Grond, P. Schulze, J. Holstein, "System Analyses Power to Gas: Deliverable 1: Technology Review";

[9] N. Piccinini, P. Cardillo, "*Gas, Vapori e Polveri a Rischio Di Esplosione e Incendio*";

[10] United States Department of Energy's Office of Power;

[11] "The Pros and Cons of Hydrogen and Fuel Cells, Production", available at: http://www.altenergy.org;

[12] S. Peantong, S. Tangjitsitcharoen, "A study of using hydrogen gas for steam boiler in Cholor– Alkali manufacturing";

[13] Heterogeneous Catalysis Research Group (HCRG), The Ohio State University, available at: https://ozkanhcrg.engineering.osu.edu;

[14] M. Ni, M. Leung, "Parametric study of solid oxide steam electrolyzer for hydrogen production";

[15] M. Santarelli, "Course of Hydrogen Technology and Fuel Cells";

[16] S. Gopalan et al., "Analysis of Self-Sustaining Recuperative Solid Oxide Electrolysis Systems";

[17] "Green Industrial Hydrogen research project", available at: http://www.green-industrial-hydrogen.com;

[18] Y. Wang et al., "A novel clean and effective syngas production system based on partial oxidation of methane assisted solid oxide co-electrolysis process";

[19] X. Sun et al., "Thermodynamic analysis of synthetic hydrocarbon fuel production in pressurized solid oxide electrolysis cells";

[20] J. Hansen, N. Christiansen, J. Nielsen, "Production of sustainable fuels by means of solid oxide electrolysis";

[21] G. Servetti, "Fuel production via co-electrolysis SOEC and syngas upgrading: a techno-economic analysis";

[22] S. Rönsch et al., "Review on methanation – from fundamentals to current projects";

[23] J. Jensen, J. Poulsen, N. Andersen, "From coal to clean energy";

[24] Haldor-Topsøe, "From solid fuels to substitute natural gas (SNG) using TREMP™";

[25] J. Schefold, A. Brisse, H. Poepke, "23,000 h Steam Electrolysis with an Electrolyte Supported Solid Oxide Cell";

[26] L. Piovan, "*Progettare Impianti a Vapore*";

[27] J. E. O'Brien et al., "Parametric study of large-scale production of syngas via high-temperature co-electrolysis";

[28] Aspen Technology Inc., "Aspen Plus User Guide";

[29] DOE/NETL, "Cost and performance baseline for fossil energy plants volume 2: coal to synthetic natural gas and ammonia";

[30] J. Porubova, G. Bazbauers, D. Markova, "Modeling of the adiabatic and isothermal methanation process";

[31] SNAM Rete Gas, "*Codice Di Rete - Allegato 11/A*";

[32] ISO 13443:1996, "Natural gas -- Standard reference conditions";

[33] M. Pozzo et al., "Enhanced Biomass-to-Liquid (BTL) conversion process through high-temperature co-electrolysis in a solid oxide electrolysis cell (SOEC)";

[34] D. Todd, M. Schwager, W. Mérida, "Thermodynamics of high-temperature, high-pressure water electrolysis";

[35] *Ministero dello Sviluppo Economico*, available at: http://dgsaie.mise.gov.it;

[36] R. Yaffee, M. McGee, "Introduction to time series analysis and forecasting";

[37] ENAMA, "Biomass and energy - availability of biomass", available at: https://www.enama.it;

[38] U. Henriksen et al., "The design, construction and operation of a 75 kW two-stage gasifier";

[39] F. Monaco et al., "Making synthetic fuels for the road transportation sector via solid oxide electrolysis and catalytic upgrade using recovered carbon dioxide and residual biomass";

[40] ENAMA, "Biomass and energy - analysis of the plants, second-generation biofuels and case studies", available at: https://www.enama.it;

[41] F. Reale et al., "*Analisi e stima quantitativa della potenzialità di produzione energetica da biomassa digeribile a livello regionale. Studio e sviluppo di un modello per unità energetiche Parte 1 – Metodologia*";

[42] ISPRA, "Report on municipal solid wastes 2015";

[43] T.Z.D. de Mes et al., "Methane production by anaerobic digestion of wastewater and solid wastes";

[44] A. Kohl, R. Nielsen, "Gas Purification";

[45] F. Bauer et al., "Biogas upgrading - review of commercial technologies";

[46] E. Mancuso, "*Inventario annuale delle emissioni di gas serra su scala regionale*";

[47] TERNA, "Power plants in Italy – 2016", available at: https://www.terna.it;

[48] M. Santarelli, A. Lanzini, "Polygeneration and advanced energy plants" course slides;

[49] M. Gatti et al., "Review, modeling, heat integration, and improved schemes of Rectisol®-based processes for CO_2 capture";

[50] ISTAT, "*Risorse Idriche Naturali per Regione*", available at: https://www.istat.it;

[51] GSE, "*Rapporto Statistico GSE Fonti Rinnovabili 2016*", available at: https://www.gse.it;

[52] A. Buttler et al., "A detailed techno-economic analysis of heat integration in high-temperature electrolysis for efficient hydrogen production".